Tectonophysics 609 (2013) 154–183

Contents lists available at ScienceDirect

Tectonophysics

journal homepage: www.elsevier.com/locate/tecto

Review Article

Crustal structure of the Siberian craton and the West Siberian basin: An appraisal of existing seismic data

Yulia Cherepanova *, Irina M. Artemieva, Hans Thybo, Zurab Chemia

Geology Section, IGN, University of Copenhagen, Denmark

ARTICLE INFO

Article history:
Received 17 August 2012
Received in revised form 22 April 2013
Accepted 7 May 2013
Available online 14 May 2013

Keywords:
Moho
Crustal structure
Seismic velocities
Siberian craton
West Siberian basin

ABSTRACT

We present a digital model SibCrust of the crustal structure of the Siberian craton (SC) and the West Siberian basin (WSB), based on all seismic profiles published since 1960 and sampled with a nominal interval of 50 km. Data quality is assessed and quantitatively assigned to each profile based on acquisition and interpretation method and completeness of crustal model. The database represents major improvement in coverage and resolution and includes depth to Moho, thickness and average P-wave velocity of five crustal layers (sediments, and upper, middle, lower, and lowermost crust) and Pn velocity. Maps and cross sections demonstrate strong crustal heterogeneity, which correlates weakly with tectono-thermal age and strongly with tectonic setting. Sedimentary thickness varies from 0–3 km in stable craton to 10–20 km in extended regions. Typical Moho depths are 44–48 km in Archean crust and up-to 54 km around the Anabar shield, 40–42 km in Proterozoic orogens, 35–38 km in extended cratonic crust, and 38–42 km in the West Siberian basin. Average crustal Vp velocity is similar for the SC and the WSB and shows a bimodal distribution with peaks at ca. 5.4 km/s in deep sedimentary basins and ~6.2–6.6 km/s in parts of the WSB and SC. Exceptionally high basement Vp velocities (6.8–7.0 km/s) at the northern border between the SC and the WSB indicate the presence of magmatic intrusions and are proposed to mark the source zone of the Siberian LIP. The cratonic crust generally consists of three layers and high-velocity lowermost crust (Vp ~ 7.4 km/s) is observed only locally. Pn velocities are generally ~8.2 km/s in the SC and WSB and abnormally high (8.6–8.9 km/s) around kimberlite fields. We discuss the origin of crustal heterogeneity and link it to regional crustal evolution.

Contents

* Corresponding author. Tel.: +45 53124833.
E-mail address: yc@geo.ku.dk (Y. Cherepanova).

0040-1951
http://dx.doi.org/10.1016/j.tecto.2013.05.004

1. Introduction

Secular evolution of the crust and the mantle is closely related, and structural and compositional heterogeneity of the crust is essentially controlled by plate tectonics and mantle dynamics. Knowledge of the origin and evolution of the continental crust is compulsory for understanding of Earth evolution in general. Information on the crustal structure is further crucial for studies of the subcrustal lithosphere and the sublithospheric mantle, given that crustal structural heterogeneities effectively mask and distort mantle compositional anomalies as reflected, in particular, in seismic surface-wave tomography and gravity models. For this reason, it is essential to correct most geophysical data for the crustal effects prior to analysis for the mantle component of the anomalies.

Direct sampling of the deep crust has limited coverage, but provides key information on the composition and physical properties of crustal rocks. Laboratory-based information on the composition of the crust originates largely from crustal xenoliths brought to the surface by magmatic events (Downes, 1993; O'Reilly and Griffin, 1985; Rudnick and Fountain, 1995; Shatsky et al., 2005) and from several, although limited in number, slices of deep crust exposed by collision tectonics and impact events, such as the Kapuskasing terrane in Canada, the Vredeford impact crater in South Africa, the Ivrea zone in the Alps, and the Western Gneiss region in Norway. Given the limited spatial crustal sampling by xenoliths and the small number of tectonically exposed crustal sections, globally the structure of the continental crust is primarily known from geophysical data. These data are chiefly based on seismic studies (initially based on reflection and refraction profiles, supplemented more recently by receiver function (RF) studies and surface wave tomography), gravity modeling, and borehole data for the shallow crust.

The vast amount of seismic data collected worldwide in different tectonic settings, since the early crustal databases (Macelwane, 1951) has led to the recognition of specific crustal structures typical for various tectonic settings; a decade later they were systematically averaged and typical crustal cross-sections were derived (Closs and Behnke, 1963). Since then, this approach has become increasingly popular, in particular due to the growing demand for global seismic studies of the (first-order, at least) crustal structure even in regions without detailed geophysical data coverage. In such regions, some first-order constraints on large-scale structural properties of the crust (such as Moho depth) can be inferred from the tectonic evolution of a particular region. Such an approach is based on the widely adopted hypothesis that the structure of the continental crust is essentially controlled by its age and tectonic settings (Jarchow and Thompson, 1989; Mooney et al., 1998). However, significant deviations from generally accepted patterns are also very common (e.g. Artemieva et al., 2006; Clowes et al., 2002). In particular, recent high-resolution seismic studies of Precambrian cratons have demonstrated the presence of highly heterogeneous crustal structure even on small scale. For example, in the Kaapvaal craton of South Africa the depth to Moho varies from 35 km to 44 km over a distance of ca. 100 km and, due to strong compositional and structural heterogeneity of the crust, these variations are poorly correlated with variations in the Poisson's ratio (Nair et al., 2006; Youssof et al., 2013–this volume). Similar observations are reported in detailed seismic surveys from other tectonic settings.

Two widely used global crustal models, CRUST 5.1 and CRUST 2.0 (Bassin et al., 2000; Mooney et al., 1998) are largely based on seismic reflection–refraction data available by 1995 (Christensen and Mooney, 1995), complemented by other data sources on the thickness of sediments. These models are constrained by statistical averaging and tectonic regionalization of the available seismic models on regular grids used to fill-in the “white spots” where data are not available and, together with a significant number of regional databases of the crustal structure, they are important tools for modeling mantle velocity and density heterogeneities. Despite unquestionable advantages provided by global crustal models, they have limitations: (1) Spatial averaging over cells with dimensions of a few hundred kilometers smears lateral variations in the crustal structure and reduces the amplitude variation of seismic velocities and thicknesses of various crustal layers, as well as total crustal thickness. The situation is similar to a low-resolution topographic map of an orogen where high peaks and deep valleys are averaged into a smooth picture. (2) Spatial averaging may lead to artifacts in regions with strong crustal heterogeneity, in particular because data acquisition often targets at tectonically “exciting”, read anomalous, structures.

Given the above limitations, the accuracy and uncertainty of the two existing global crustal models cannot be assessed, even though they have been indirectly tested by global tomographic inversion (e.g. Mooney et al., 1998). For Siberia, the sparse sampling by teleseismic data prevents such a test, as it will be basically unconstrained by seismic data. The accuracy of the CRUST 2.0 model in each cell is estimated to be within 1.0 km for the sediment thickness and within 5 km for the crustal thickness (http://igppweb.ucsd.edu/~gabi/crust2.html). It is also clear that regional high resolution geophysical modeling requires high resolution regional crustal models. Additionally, such regional crustal databases would provide critical information for verifying the accuracy of global crustal models, updating the global statistics on the crustal structure that forms their basis, and potentially updating the global crustal models.

This study reports a new, independent compilation of the crustal structure of Siberia, SibCrust, based on all available seismic models for the region. The study area is limited to the area 60-132E and

50N–75N, and includes two major tectonic provinces, the largely Paleozoic West Siberian basin (WSB) and the Precambrian Siberian craton (SC). It extends from the Ural mountains in the west to the Lena river and the Verkhoyansk Ridge in the east, and from the Arctic shelf in the north to the Central Asian mountain belt in the south (Fig. 1).

We provide a brief history of seismic studies in Siberia, followed by a summary of seismic data coverage, a description of the database structure, and a description of the adopted quality criteria for seismic data acquisition and interpretation. Maps and histograms illustrate the database and are used as background for discussion of major features of the crustal structure in the West Siberian basin and the Siberian craton, which we link to the tectonic evolution of the region over ca. 3.6 Ga. The compiled database is analyzed statistically in relation to crustal age and is compared to results from other regions with similar tectonic settings.

2. Seismic data coverage in Siberia

2.1. An overview of regional seismic surveys

A systematic study of seismic structure of the crust using a wide range of DSS (deep seismic sounding) techniques began in the Soviet Union in the early 1950s (Table 1). DSS profiles recorded in some parts of Eastern (SC) and Western (WSB) Siberia prior to the 1960s were shorter than 300 km. In the late 1960s, the differential seismic sounding (pseudo 3D sounding) method was applied in a large exploratory seismic study of the southern West Siberian basin and in an areal study of the Siberian craton Puzyrev and Krylov (1977). The number of high resolution DSS profiles increased in the 1970–1980s, although low resolution DSS profiling still dominated. High resolution seismic profiling, initiated in the late 1970s, was initially carried out mainly along short profiles designed for crustal studies only and often only for the sedimentary cover.

Between 1965 and 1988, 122 peaceful nuclear explosions (PNE) were detonated in the USSR for different scientific applications (Sultanov et al., 1999). The major part of the PNE program was a deep seismic survey on a network of long range geotraverses (3000–4500 km long seismic profiles) that cross diverse geologic structures of Eurasia and provide unique information on the deep crustal and mantle structure down to 700 km depth (Mechie et al., 1993; Morozova et al., 2000; Thybo et al., 2003a), and in a few cases even to the core–mantle boundary (Thybo et al., 2003b). Chemical shots were additionally used along the PNE profiles as source to obtain crustal structure along the same profiles. The technical parameters, such as the number and spacing of chemical shots and recorders, together with progress in instrumentation and in interpretation methods determine the quality

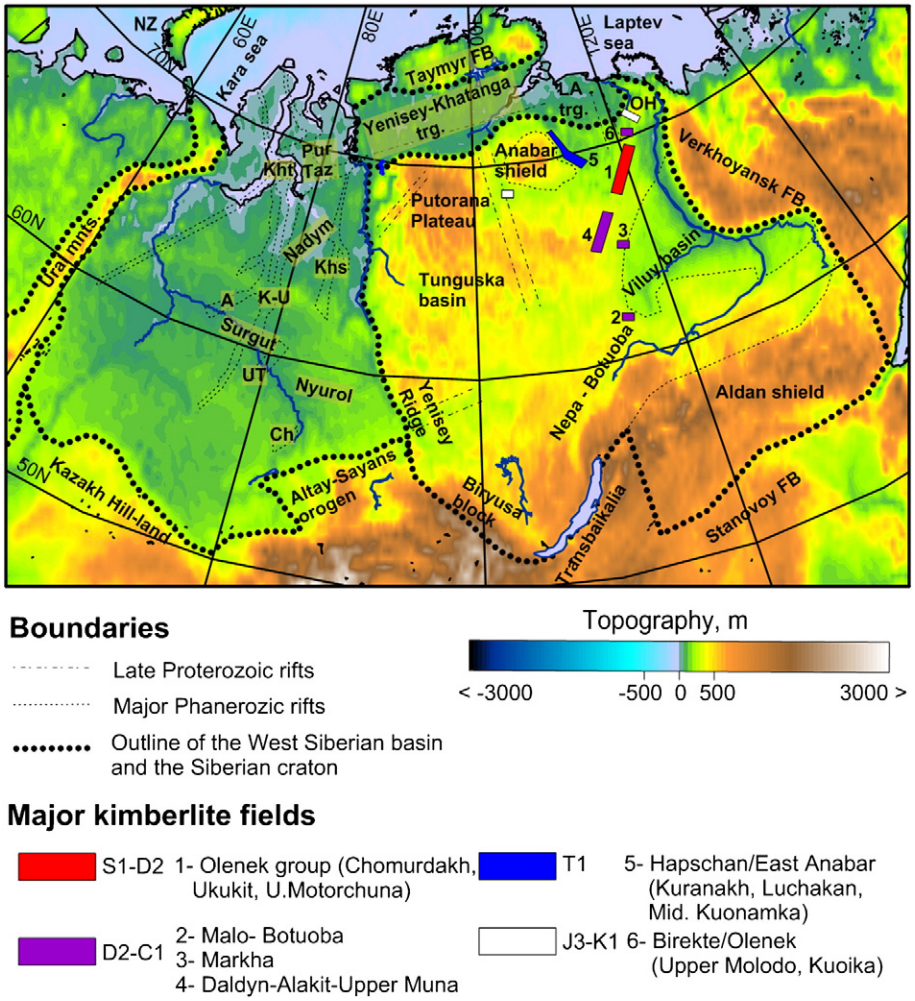

Fig. 1. Topography of the West Siberian basin (WSB) and the Siberian craton (SC) based on ETOPO1 (Amante and Eakins, 2009). The map shows the boundaries of the WSB and the SC, the known and suspected Proterozoic and Paleozoic rift-graben structures (after Aplonov, 1995; Pavlov, 1995; Surkov and Smirnov, 2003; Zonenshain et al., 1990), major sedimentary basins and basement highs, relict oceanic basins of the WSB (Nadym, Surgut, and Nyurol), and major kimberlite fields of the SC. Abbreviations for rift-grabens of the WSB: A, Agan; Ch, Chuzik; K–U, Koltogory–Urengoi; Khs, Khudosei; Kht, Khudottei; UT, Ust–Tym. Other abbreviations: LA trg.—Lena–Anabar trough; NZ—Novaya Zemlya; OH—Olenek High; FB—fold belt. The letter and color code for the kimberlite fields refer to the emplacement age (S1 = 420 Ma, D2 = 380 Ma, C1 = 340 Ma, T1 = 245–240 Ma, J1 = 170 Ma, K1 = 140 Ma) (after Griffin et al., 1999).

Table 1
Classification of seismic models by the acquisition and interpretation method.

	Acquisition method		Details of acquisition parameters	Label in database	Quality	Total length of seismic profiles, km
Profile acquisition method	Short range profiles (<500 km)	High resolution reflection–refraction	Dense system of reversed and overlapping profiles, either i. Crustal refraction/wide-angle reflection profiles with reversed coverage, 2–10 km receiver spacing, chemical shots as source, 10–100 km distance between shot points, interpreted with primary and secondary arrivals; or ii. Multichannel normal-incidence reflection profiles with 24 or 48 channels, 50–200 m receiver spacing, chemical shots as source, 1–3 km between shot points.	DSS-A	A	ca. 12,000
		Low resolution reflection–refraction	i. Geometry as in DSS-A with less dense receiver spacing or gaps in array coverage; model resolution is lower than for DSS-A profiles. ii. Experiments with several widely spaced stations, each with 24 or 48 receivers spaced 50–200 m to provide apparent velocity of individual phases.	DSS-B	B	ca. 5700
		Pseudo 3D sounding	Source and three or four arrays of receivers (trace spacing 2–10 km) that were moved along the profile while maintaining the same configuration. Wave field registration at different offsets from the source for different layers (30–60 km for the basement; 100–200 km for Moho depth; 200–300 km for Pn). Registration of refracted, reflected and converted waves	DSS-C	C	ca. 11,960
	Long range profiles (>500 km)	Combination of DSS profiling methods	Long-range PNE profiles, 2000–3000 km long, covered by 200–300 receivers for mantle studies with 2–4 nuclear sources (PNE) per profile.	LRDSS-A	A	ca. 22,000
			Crustal models along the same profiles are based on additional chemical shots with 30–40 km spacing with data acquisition along 350–400 km long profiles with a 40–50 km overlap between individual profiles. Receiver spacing: 3–10 km along the whole length of profiles. Receivers: 3-component stations "Taiga" and "Cherepaha". Model quality depends on interpretation method. LRDSS-A: high quality modern, ray-tracing based interpretations; LRDSS-B: lower quality original interpretations with limited computer processing.	LRDSS-B	B	ca. 5000
	Receiver function method		Time series calculated by rotation and deconvolution of three-component seismograms to show the local seismic response of Earth structure near the receiver. Provides mainly information on Moho depth with 2–4 km uncertainty because crustal velocities rarely are known, rarely provides information on internal crustal structure, and only average crustal velocity.	RF	C	ca. 1630
Total length of seismic profiles (km):						ca. 58,000

of the crustal seismic models (Table 1). Consequently, the resolution of the crustal structure significantly differs between and even along the PNE profiles (Figs. 2, 3).

A significant strength of the DSS studies in the USSR was standardization, both in experimental techniques and in interpretation, since they were carried out by a small number of research groups (e.g. Ryaboy, 1989). This led to a systematic program of seismic exploration of the entire country and not only in regions of economic potential. An unquestionable advantage of the Soviet seismic program is the reversed and overlapping profiling method which allows direct interpretation of laterally heterogeneous structure. A weakness is that interpretations of the very early studies are available only as low quality graphical presentation of the results (i.e. maps are schematic, with only few details and often without coordinates and scales, the cross sections are hand-drawn, and the seismic data are interpreted without use of computer-based ray tracing; the latter two concerns are also the case for other contemporaneous seismic interpretations worldwide).

2.2. Previous compilations of crustal structure

The first compilations of regional crustal databases for Siberia go back to the 1970s and 1980s and are available as maps showing the thickness of sediments and the Moho depth (Bazanov et al., 1976; Belyaevsky, 1973; Kontorovich et al., 1975; Kovylin, 1985; Kunin and Ioganson, 1984; Rudkevich, 1974; Savinsky, 1972). These crustal maps are based not only on the available seismic data but also include borehole data for the sedimentary cover and potential field constraints for areas which were not covered by seismic surveys. These original maps have been reproduced, with minor modifications, in numerous later publications, often without credit to the original maps. Over the past 30–40 years, significant advances have been made in seismic studies by development of data acquisition and interpretation methodologies (Tables 1, 2). The coverage of Siberia by seismic surveys and deep drilling has also significantly improved since the first regional crustal models were derived. Surprisingly, major features of the crustal and sedimentary thickness variations have been correctly recognized already in those early regional crustal models.

There are three relatively recent (and, in general, not publically available) crustal compilations for the territory of Siberia. (1 & 2) Two very similar compilations of Russian geological surveys, GEON and VSEGEI (Erinchek, 2009; Kostyuchenko, 2000), include only data on the thickness of the sedimentary cover, depth to Moho, and Pn velocity, without information on the velocity structure of the crust. These compilations, available as interpolated maps, represent a development of the crustal models of the 1970–1980s and are based on a combination of seismic and potential field constraints, complemented by borehole data and tectonic information. An advantage of the approach is that the entire territory, including

areas without seismic data coverage, is included into the crustal model. However, a significant disadvantage is that such compilations cannot be applied for gravity modeling, given that a significant part of the crustal structure is derived from the gravity field.

(3) In contrast to the compilations of VSEGEI and GEON, a continuing USGS compilation of seismic profiles worldwide (Mooney and Detweiler, 2005) also includes detailed information on the velocity structure of the crust. Seismic profiles included in this database by the mid-1990s formed the basis for the coverage of Siberia in the two global crustal models, CRUST5.1 and CRUST2.0 (Bassin et al., 2000; Mooney et al., 1998). Specifics of Soviet publications cause problems in the USGS compilation for the territory of Russia. Firstly, the results of many Soviet seismic surveys were published only in annual or field reports of various national organizations and are not generally available and thus are not included into the compilation. Secondly, even publications of seismic profiles in scientific journals usually do not provide their exact location. As a result, many Soviet seismic profiles are missing in the USGS database or are significantly misplaced (in some cases by some hundreds of kilometers, as in case of the ultra-long range PNE profiles). An inclusion of any published crustal model, without quality assessment, into a compilation also has a drawback, in particular with respect to the velocity structure of the crust as reported in the early studies (for details see Section 3). Our compilation compensates to a large degree for all these problems.

Our study was provoked by a significant discrepancy between the crustal models of Siberia as demonstrated by a comparison of the compilations of VSEGEI, GEON, and USGS. Differences amount to 10 km for Moho depth and 1–3 km for the thickness of sediments. These differences may lead to systematic errors when used in surface wave tomography models and potential field modeling. Consequently, the use of these models for the crustal structure of Siberia may question the results of recent geophysical studies, such as the gravity modeling results for the West Siberian basin (Braitenberg and Ebbing, 2009) and the seismic tomography model of the West Siberian basin and the Siberian craton (Priestley and Debayle, 2003). This situation motivated us to initiate a new compilation of the crustal structure of Siberia from scratch, without making use of any previous compilation.

3. New database of the crustal seismic structure, SibCrust

Our goal is to constrain a trustworthy regional crustal model, justified by available and reliable seismic models. To avoid the problems of previous compilations, we have adopted the following strategies (see details below):

- to digitize all available and reliable seismic models for the region;
- to apply quality criteria as defined by seismic data acquisition and interpretation methods;
- to exclude models with uncontrolled quality and uncertainty such as crustal models for regions without seismic data, crustal models based on gravity modeling and/or tectonic similarities, and crustal models published as interpolated contour maps but not along seismic reflection/refraction profiles.

3.1. Data sources and digitizing strategy

The data set used in the compilation includes all available published seismic reflection, refraction and receiver function interpretations of regional seismic data acquired since the late 1960s until present (Table 3). To ensure full coverage of the existing seismic profiles in Siberia, the locations of digitized profiles were compared with the all-Russian compilation of seismic profiles by VSEGEI (Erinchek, 2009). Our new crustal database includes almost all (except for a few very old and publically unavailable) seismic profiles that exist for Siberia with the total length of digitized profiles ca. 58,000 km.

The new crustal database is based on approximately 50 publications. Importantly, this small number does not reflect the total number of publications that we have used, which is several times larger. It includes the vast number of research articles published since the 1970s in Russian and international scientific journals and

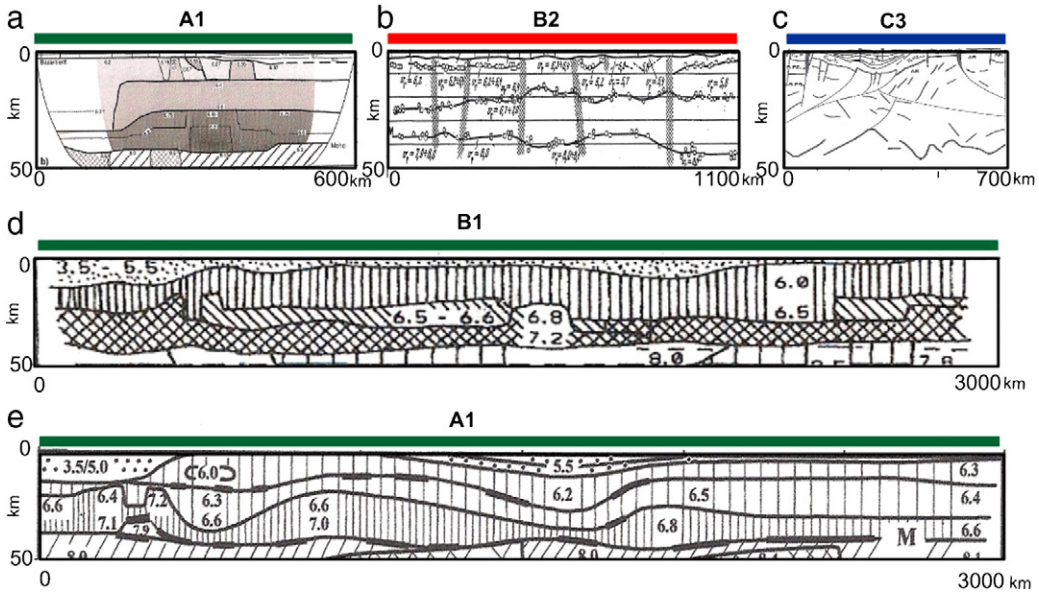

Fig. 2. Examples of published seismic models illustrating model quality criteria adopted in this study (see Tables 1–2 for details). Color codes and numbers (1 to 3) refer to the completeness of model information on the crustal inner structure and are the same as in Fig. 3: green (1)—complete, red (2)—intermediate, blue (3)—incomplete model. Letter codes refer to the quality of seismic model based on interpretation method and quality of data acquisition (A—high, B—intermediate, C—low; see details in Table 1). (a) An example of a profile with a complete crustal information and high quality acquisition and interpretation (profile 1 in Table 3, Suvorov et al., 2006). (b) An example of an average quality profile with partial crustal information (profile 6 in Table 3, Zverev and Kosminskaya, 1980). (c) An example of a poor quality profile with incomplete information on the crustal inner structure and low quality of seismic model (profile16 in Table 3, Kostyuchenko, 2000). (d, e) Two crustal models for the long-range PNE profile RIFT (profile 30 in Table 3) based on the same seismic data illustrating differences in seismic models interpreted at different time: (d) the model of Egorkin et al. (1987); (e) ray tracing interpretation by Pavlenkova et al. (2002).

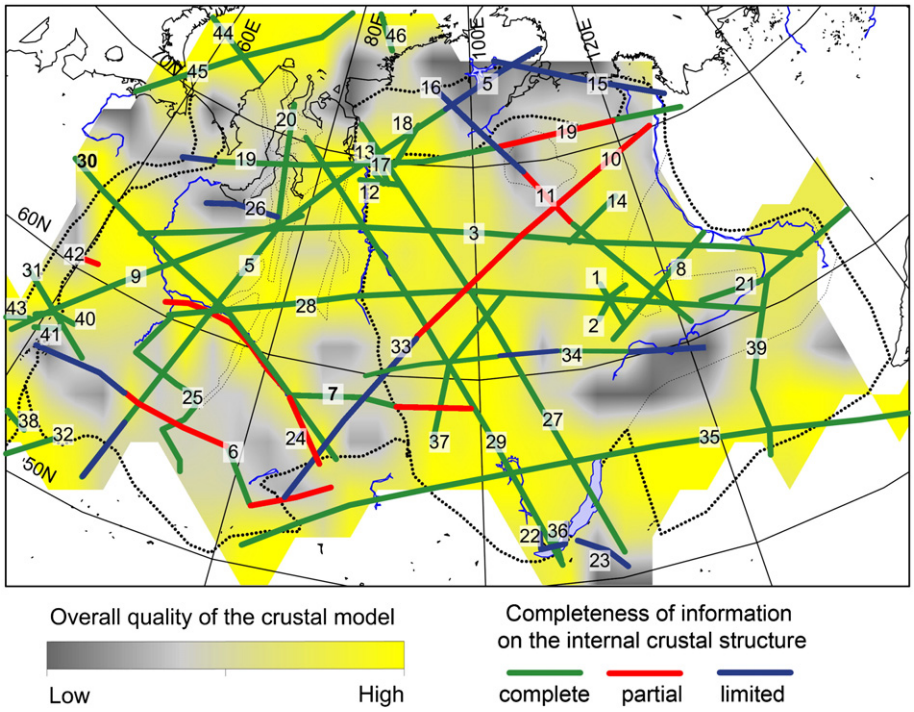

Fig. 3. Overall quality of the crustal database based on available seismic models. Shading illustrates the overall quality of the crustal model based on both model quality (criteria A–C) and model completeness (criteria 1–3). This information is presented for a 2° × 2° interpolation grid which corresponds to interpolation procedure used to constrain all other maps. Seismic profiles which were included into the database are numbered according to Table 3 where typical model quality is given for each profile; color code shows the completeness of model information on the crustal inner structure along the individual profiles (see Fig. 2 for examples and Section 3.3 for details).

books, as well as numerous open-file reports and dissertations from various Russian organizations, including a few models from the 60s when no later interpretations are available. Note that publications which reproduce (sometimes several times by the same authors) seismic models with no or only minor changes as compared to the first original publication are excluded from our reference list. Several publications present interpretations of many seismic profiles, such that the total number of profiles is larger than the number of original publications.

For many seismic profiles, several (and sometimes notably different) seismic models constrained by different research groups are available. In such cases, only one seismic model per profile is incorporated into the database and selected from reliability criteria (see below), although in some cases our choice is inevitably subjective. Commonly, when several crustal models are available the most recent interpretations were preferred, since generally they are of higher quality (Fig. 2). In general, the old interpretations of Moho depth are in a good agreement with the most recent interpretations, but the details of the crustal structure may notably differ. Recent interpretations of the old seismic data demonstrate the high quality of the original seismic material and its high potential for a high resolution interpretation (Morozov et al., 2002; Suvorov et al., 2005, 2006).

3.2. Structure of the database

Following both seismic practice and petrologic structure of a typical continental crust, the new crustal model SibCrust consists of five layers: sediments, the upper crust, the middle crust, the lower crust, and the high-velocity lowermost crust (where recognized). Additionally, the Pn velocity at the top of the upper mantle is included. Each layer is characterized by two parameters: thickness and average P-wave velocity. Thus, each entry in the database is specified by 11 parameters which describe the crustal structure at that location. The subdivision of the crustal structure into the crustal layers is largely based on the typical Vp velocities as reported in global and regional crustal models:

- <5.8 km/s in sedimentary strata (note that the commonly adopted boundary value of 5.6 km/s is not used because of widespread occurrences of limestones with Vp = 5.4–5.7 km/s),

Table 2
Major seismic data acquisition and interpretation campaigns.

Years of acquisition	Prior to 1976	1976–1985	After 1985
Acquisition method	Low-resolution DSS pseudo 3D sounding	High resolution DSS and Long range PNE profiles	High resolution DSS, normal incidence reflection profiling and broad band seismometers
Recording technique	1-component recording system	3-component receivers, analog stations	3-component geophones and broad band seismometers, digital stations
Source type	Chemical shots	Chemical shots and nuclear shots	Chemical shots Earthquakes
Interpretation	1-D models; head (refracted)-wave method; systematic velocity overestimation at intracrustal boundaries (before 1970)	2-D models; ray-tracing method based on reflected and refracted waves; velocity filtering, high lateral and vertical resolution	2-D models; ray-tracing method; seismic tomography (crustal), reflection seismic processing, receiver functions

Table 3
Seismic profiles available for the region and included into the database.

Profile number in database/ profile name if available	Year of field work	Profile length (km)	Quality rate[a]	Seismic source	Maximum resolved depth	Key reference[b]	Additional references[c]
1 SC, Mirny	1981	370	A	CS	Moho	Suvorov et al. (2006)	
2 SC, Mirny	1983	340	A	CS	Moho	Suvorov et al. (2006)	
3 Craton WSB-SC	1978	3000	B	CS + PNE	400 km	Pavlenkova and Pavlenkova (2006)	Egorkin et al. (1987), Romanyuk (1995), Pavlenkova et al. (1996), Solodilov (1997), Nielsen et al. (1999), Egorkin (1999), Petrov and Kostyuchenko (2002)
4 Quartz Ural-WSB	1984	3950	A	CS + PNE	400 km	Beloussov et al. (1991), Morozov et al. (2002)	Egorkin (Yegorkin) et al. (1992), Mechie et al. (1993), Kostuychenko and Egorkin (1994), Ryberg et al. (1996), Schueller et al. (1997), Morozov et al. (1998), Egorkin (1999), Pavlenkova (2000), Pavlenkova and Pavlenkova (2006)
5 Bitum WSB-SC	1983	3300	A	CS + PNE	400 km	Beloussov et al. (1991)	
6, 7 WSB	1969	1950, 1900	C	CS	Moho	Zverev and Kosminskaya (1980)	Krylov et al. (1974a,b), Puzyrev and Krylov (1977)
8 SC	1977	850	B	CS	60 km	Zverev and Kosminskaya (1980)	
9 Rubin 2 WSB	1983–1990	1800	B	CS	Moho	Bulin (2003)	
10 Shpat	1983Q	1950	B	CS + PNE	Moho	Bulin (2003)	
11 Oka, SC	1977	1200	A, C	CS + EQ	Moho	Bulin (1988)	
12 Norilsk region	1981	255	A	CS + EQ	Moho	Avetisov and Golubkov (1984)	Avetisov and Golubkov (1996)
13 Norilsk region	1981	55	C	EQ	Moho	Avetisov and Golubkov (1984)	
14 Northern SC	1980	420	A	CS	Moho	Suvorov et al. (2005)	Suvorov (1993)
15 Northern SC	1983	650	C	EQ	Moho	Kostyuchenko (2000)	
16 Northern SC	1981	925	C	EQ	Moho	Kostyuchenko (2000)	
17 Norilsk region	1988	200	A	CS	Moho	Bulin and Egorkin (1994)	
18 Northern SC	1988	240	B	CS + EQ	Moho	Bulin and Egorkin (1994)	
19 Horizont, Northern WSB-SC	1976	2600	B	CS + PNE	400	Zverev and Kosminskaya, 1980	Pavlenkova and Pavlenkova (2006)
20 Northern WSB	1976	930	C	CS	Moho	Zverev and Kosminskaya (1980)	
21 Viluy, SC	1969	580	C	CS	Moho	Vol'vovsky and Vol'vovsky (1975)	
22 Baikal	1969	730	C	CS	Moho	Vol'vovsky and Vol'vovsky (1975)	
23 Baikal	1969	750	C	CS	Moho	Vol'vovsky and Vol'vovsky (1975)	
24 Southern WSB	1969	700	C	CS	Moho	Vol'vovsky and Vol'vovsky (1975)	
25 Southern WSB	1969	1080	C	CS	Moho	Vol'vovsky and Vol'vovsky (1975)	Gao et al. (1994), Zorin et al. (1995)

26 Northern WSB	1969	500	C	CS	Moho	Vol'vovsky and Vol'vovsky (1975)	
27 Meteorite SC	1978	2800	A	CS + PNE	400	Pavlenkova and Pavlenkova (2006), Salnikov (2008)	Pavlenkova et al. (1996), Egorkin (1999)
28 Kimberlite, Central WSB-SC	1978	2900	A, B, C	CS + PNE	400	Pavlenkova and Pavlenkova (2006)	Egorkin et al. (1987), Salnikov (2008), Grachev and Kaban (2006)
29 Rift, SC	1985	3000	A	CS + PNE	400 km	Pavlenkova et al. (2002)	Egorkin et al. (1987), Pavlenkova (1998), Salnikov (2008)
30 Quartz, the Urals segment	1987	620	A	CS + PNE	400	Kostuychenko et al. (1998)	
31 Rubin, northern Middle Urals	1990	800	A	CS + PNE	Moho	Kostuychenko et al. (1998)	Egorkin (1991)
32 South Ural	1989	830	A	CS + PNE	Moho	Kostuychenko et al. (1998)	
33 Shpat	1983	1500	B	CS + NPE	Moho	Ryaboy (1989)	
34 SC	1970	1070	C	CS	Moho	Salnikov (2008)	
35 Basalt	1985/2000	4000	A	CS + PNE	Moho	Egorov et al. (2000)	
36 Baikal	2003	360	A	CS	Moho	Thybo and Nielsen (2009)	Zorin et al. (2002)
37 SC, west	???	850	A	CS	Moho	Surkov et al. (2000)	
38 URSEIS, Southern Middle Urals	1995	350	A	CS	Moho	Brown et al. (1998), Carbonell et al. (2000)	Steer et al. (1995, 1998), Echtler et al. (1996), Puchkov (1997), Carbonell et al. (1996), Suleimanov (2006)
39 3-DV, Far East	???	2200	B	CS	Moho	Salnikov (2008) Salnikov et al. (2012)	
40 ESRU R-114/115, northern Middle Urals	1993–1998	260	A	CS	Moho	Juhlin et al. (1996)	Druzhinin et al. (1990, 1997), Sokolov (1993), Juhlin et al. (1998), Brown et al. (1998, 2002), Friberg et al. (2001), Kashubin et al. (2006), Knapp et al. (1998), Brown et al. (2008)
41 UWARS, northern Middle Urals	1992	170	A	CS	Moho	Thouvenot et al. (1995)	
42 R-17, Northern Urals	1993	70	C	CS	Moho	Juhlin et al. (1996)	Egorkin (1991), Ryzhiy et al. (1992)
43 Granit, the Middle Urals segment	1990–1992	3000 (400 km)	A	CS	Moho	Juhlin et al. (1996)	Rybalka and Kashubin (1992), Ryzhiy et al. (1992)
44 AR-2, Polar Urals	1995–2006	900	A	CS	Moho	Ivanova et al. (2006, 2011)	Roslov et al. (2009)
45 AR-3, Polar Urals	1995–2006	2500	A	CS	Moho	Ivanova et al. (2011)	
46 AR-4, Kara sea	1995–2006	2500	A	CS	Moho	Ivanova et al. (2011)	

CS—chemical shots, PNE—nuclear peaceful explosions, EQ—earthquake source.

[a] Quality—see details in Table 1. Profile locations and their quality as marked here are shown in Fig. 3.

[b] Key reference—publications from which seismic models included to the database were primarily digitized.

[c] Additional references—publications (i) where the same seismic models as in the key reference, or their parts, were republished, with no or only minor modifications, (ii) with older and less reliable interpretations based on the same seismic data as seismic models in the key reference, (iii) where the same seismic models as in the key reference, or their parts, are presented as a geological, compositional, or density interpretation. The information from additional references was occasionally used as supportive material (e.g. to better constrain profile location).

- 5.8–6.4 km/s in the upper crust (UC),
- 6.4–6.8 km/s in the middle crust (MC),
- 6.8–7.2 km/s in the lower crust (LC), and
- 7.2–7.8 km/s in the lowermost crust (LMC).

In cases where seismic reflectors are observed from refraction-wide-angle reflection surveys, we adopted the crustal layers as identified in the original studies regardless of Vp velocity values in the layers.

Seismic models were digitized along the profiles (see Fig. 3 for data coverage) with a sampling step of 50 km where the crustal structure is smooth, and denser in regions with short wavelength variation in any of the crustal properties. This procedure ensures that the spatial resolution of the database is comparable with the resolution of the original seismic models. Cross-points between seismic profiles are a special problem. At some cross-points (the most notable is near Norilsk, at ca. 88E/70N), seismic models based on data acquired and interpreted at significantly different time or by different groups, do not agree and may differ by up to 10 km for the crustal thickness. Although one cannot exclude some effect of anisotropy, in such places we primarily use the most recent interpretation for the crustal structure at cross-points (clearly, the results based on ray-tracing are preferred to old interpretations) and avoid duplicate crustal models for the same location.

3.3. Criteria adopted for quality control of the seismic model

Seismic data for Siberia, as for any other region, are of uneven quality due to objective data acquisition differences and subjective interpretation limitations. Therefore information on model quality requires special attention, and it is incorporated into the new database. Generally, the depths to the top of the basement and Moho are the most reliable parameters determined in the earliest and all consequent seismic models.

The reliability of the crustal structure (seismic models) is essentially different for data acquired at different time and interpreted by different methods. For this reason, as our first-order approach, the quality of digitized seismic models is assessed by the time of data acquisition field campaigns and by the time and method of data interpretation. Based on the combination of these two factors, each point digitized from a seismic profile is assigned a subjective quality index on a scale from A (the highest) to C (the lowest) (the details are specified in Table 1, quality typical for each digitized profile is indicated in Table 3). An additional quality parameter, on a scale from 1 (the highest) to 3 (the lowest), is used to characterize the completeness of the crustal model at each digitized point (Fig. 3). The criteria adopted for assessment of quality and completeness of seismic model are briefly discussed below and are further illustrated by four examples (Fig. 2).

(1) Time and method of data acquisition (Table 2). Most of the earliest (prior to mid-1970s) data acquisition was carried out with 1-component recorders and poor lateral resolution. While the inner crustal structure is poorly resolved in these profiles (intracrustal boundaries are often discontinuous, with lateral gaps up to 250–300 km), the depths to the Moho and the top of the basement are resolved well with an accuracy of 1–2 km (Fig. 2a). Later acquisition campaigns, defined by new exploration tasks, built on technical progress in both automation and processing and resulted in better constrained crustal models (Fig. 2b).

(2) Time and method of data interpretation (data processing methods) (Table 1). The earliest (pre-1970) interpretations were 1-D, and often involved a systematic interpretation error because secondary (sometimes sub-critical) reflections were interpreted as refracted (head) waves (assigned quality C). The result is a systematic overestimation of mid-crustal velocities. The arrival times were used for tracing crustal boundaries and for estimating layer velocities from their slopes; these velocities were then equated to the velocities in the strata down to the next crustal boundary. As a result, these velocities are also higher than the true layer velocities. For example, the old sections often indicate seismic Vp velocities of 6.8–7.0 km/s in the middle part of the crust instead of the, later interpreted, characteristic velocities of 6.4–6.5 km/s. Fortunately, new publications on the velocity structure help in the identification of such errors. The accuracy of depth determinations of seismic boundaries and the velocities of elastic waves constrained in the early surveys by pseudo 3-D DSS (termed “point soundings” in Russian literature, quality C) can be assessed from a comparison with the results of drilling and high-resolution continuous seismic profiling made under various conditions. In general, the accuracy is 0.1–1.0 km for the basement depth and 2 km for the depth to Moho and internal crustal boundaries. The accuracy of seismic P-wave velocity is 0.1–0.25 km/s (Krylov et al., 1974a), which corresponds to the accuracy of high resolution DSS (quality A, Table 1). For one profile (C9 in Table 3) where crustal structure is complete but only S-wave speed is available, Vs is converted to Vp by assuming Vp/Vs = 1.75. This profile, despite a high quality model interpretation, is considered here as of average quality since the true Vp/Vs ratio along that profile is unknown.

(3) Model completeness (Fig. 3). Completeness of digitized seismic models on the inner structure of the crust means availability of information on thickness of individual crustal layers and their Vp velocity at each digitized point. High completeness (index 1) is assigned to the points with complete information, i.e. where thickness and Vp velocity are known of all crustal layers: sediments, upper crust, middle crust, lower crust, lowermost crust (if present), Moho depth, and Pn velocity. Intermediate completeness (index 2) is assigned to points with information on the depth to the top of the basement and the Moho, with at least one intracrustal boundary, as well as with partial velocity information. Finally, low completeness (index 3) is assigned to points where only the depth to the top of the basement and the Moho are resolved. Depending on original survey geometry and interpretation approach, the internal crustal structure may be well resolved even on some average quality profiles. Since crustal models based on Receiver Function method usually do not constrain internal velocity structure of the crust and have ca. 2–4 km uncertainty for the Moho depth when the velocity structure is not known, they are assigned low quality (C) and poor completeness (3).

The three upper profiles in Fig. 2 illustrate the difference in the completeness of information on crustal inner structure. Many old interpretations (exemplified by Fig. 2c) could not resolve the structure, while improvements in signal processing over the last decades have resulted in a significant improvement of the quality of seismic modeling and interpretations, even for interpretation of old, recently digitized data (Fig. 2a). The lower profiles (Fig. 2d,e) illustrate differences in quality of seismic models, based on the same seismic data, but constrained by different interpretation methods. The high quality profile (Fig. 2e) interpreted by modern ray method was included into the database, whereas the same profile with a more detailed information on the inner crustal structure (Fig. 2d) was interpreted by hand, has lower quality, and therefore is used only as a supplementary information.

The overall quality of the entire database is assessed based on the combination of the above mentioned criteria (Fig. 3). The parameter which characterizes quality of digitized seismic models is interpolated with a 2° radius, which corresponds to the interpolation used to produce all other maps. The lowest accuracy in the resolution of the crustal structure is for the north-eastern part of the Siberian craton where available seismic models have limited quality and completeness.

There is also insufficient seismic information for the south-eastern part of the SC and some parts of the WSB (Fig. 3). As a consequence, the SibCrust model may be unreliable in these regions.

On the whole, the relatively many high quality seismic models available for Siberia (ca. 80% of the database by profile length) provides the basis for our high quality, the new regional crustal model. Average and low quality models each make ca. 10% of the database. Similar statistics exists for the completeness criteria. The exclusion of crustal models with uncontrolled and unknown errors and uncertainties (e.g. seismic models published as interpolated contour maps but not along seismic reflection/refraction profiles or models based on gravity modeling and/or tectonic similarities) from the compilation allows for maintaining strict quality control of the new regional crustal database.

3.4. Interpolation procedure for map presentation of the database

The new crustal database, SibCrust, constrained with at least 50 km spacing along all existing seismic profiles, is presented as a series of maps to illustrate variations in the thickness of sediments, depth to Moho, thickness of individual crustal layers, average velocity structure of the entire crust and the crystalline basement, and upper mantle Pn velocity. The digitized point data, representing the original 2D crustal models were interpolated on 0.5°×0.5° and 2°×2° grids for each crustal parameter in the databases. The interpolation algorithm was chosen after a comparison between different techniques (such as standard krigging). In all cases, the nearest neighbor algorithm was used as interpolation method, since it provides better amplitude preservation, particularly of small-size, high-amplitude anomalies, which is important in the tectonically complex and geologically heterogeneous region. Interpolated values were verified with the original seismic models; strongly distorted values were corrected in accordance with seismic models available within a 100 km radius.

In some low quality profiles, the internal crustal boundaries are discontinuous with lateral gaps up to 200–300 km. Such gaps in crustal parameters are filled with information from the closest (sometimes crossing) high quality profiles, if nearer than 100 km. In rare cases, with large data gaps, the standard average velocity of the crustal layer is assigned to points with incomplete velocity information. In regions with several closely spaced or intersecting crustal profiles, weighted interpolation is used, with the weight factor corresponding to the model quality (Table 1).

Given the relatively dense data coverage over the entire Siberia, there is no need to incorporate geologic/tectonic information into the interpolation; consequently the maps presented below can be directly compared to geological and tectonic structure of the region. Some major tectonic structures (the Viluy rift, the Anabar and Aldan–Stanovoy shields) are crossed by few seismic profiles only; for this reason their areal extent as reflected in the crustal maps is not fully constrained.

Crustal parameters are publically available at both grids. Small interpolation radius produces minimum artifacts, but leaves “white spots” in regions without seismic coverage. Interpolation on a uniform 2° × 2° grid is a compromise between filling the gaps without crustal information and preserving the amplitudes and, where applicable, the shapes of the anomalies. All maps shown in this paper are produced with 2° × 2° interpolation of the corresponding crustal parameters. The uncertainty associated with such type of interpolation is analyzed in detail in the companion paper (Artemieva and Thybo, 2013–this volume).

4. Overview of regional tectonic evolution

4.1. Major tectonic elements

4.1.1. The Siberian craton (SC)

The Siberian craton (SC) occupies an area of ca. 4×10^6 km^2, although the western and northern boundaries are not well established and may extend below the sedimentary covers of the West Siberian basin and the Yenisey–Khatanga trough. The basement consists of Archean and Proterozoic blocks of various origin (continental terranes, orogenic belts, magmatic arcs) separated by Proterozoic suture zones (Fig. 4). It is exposed in a few areas only: (i) the Anabar Shield in the north-central part; (ii) the Olenek High in the north-eastern part; (iii) the Yenisey ridge in the west; (iv) two areas in the Biryusa block in the south-west of SC; (v) the Aldan–Stanovoy block in the south-east. The boundaries of the crustal blocks are constrained chiefly by magnetic anomalies and isotope ages (Rosen, 2002) as most of the craton is covered by a thick layer of Riphean–Phanerozoic sediments and by Permo-Triassic flood basalts in the north-west.

4.1.2. The West Siberian basin (WSB)

The West Siberian basin (WSB) is a gigantic sedimentary basin that extends ca. 2500 km from north to south and 1000 to 1900 km from west to east and covers an area comparable to the Siberian Craton (~3.5×10^6 km^2). The thick sedimentary cover of the WSB hosts some of the world's largest natural gas and oil fields below an almost flat topography. The WSB is bounded by Paleozoic-Mesozoic orogens in the west, south, and southeast, and by the Siberian craton in the east. The northern extent of the WSB forms a shelf that extends for more than a thousand kilometers into the Arctic ocean. The tectonic origin of the shelf is presently under intensive investigation, and it is thought to consist chiefly of a Neoproterozoic fold belt (Drachev et al., 2010).

Potential field data indicate that the basement of the WSB is a collage of terranes ranging in age from 1800 to 1600 Ma to the Mesozoic. Up to eight buried Precambrian blocks are interpreted in the basement of the central and southern West Siberian basin, mostly from potential field studies (e.g. Aplonov, 1995). The Uvat–Khantymansiysk median massif is the largest (Figs. 5, 6) and is often described as a (Meso-)Proterozoic microcontinent (Bekzhanov et al., 1974). However, isotope ages are sparse and the exact age and size of this lithospheric block are highly speculative (Surkov and Smirnov, 2003). Data from at least 30 deep boreholes that reach the WSB basement provide evidence for Proterozoic (chiefly undefined) basement ages along the northern margin of the WSB (Aplonov, 1988, 1995; Bochkarev et al., 2003; Peterson and Clarke, 1991; Surkov and Zhero, 1981). The oldest absolute age of ca. 750 Ma is reported at the south-western part of the Ob Guba bay (ca. 64–68N/64–72E) and basement ages of ca. 650–500 Ma are reported for the north-eastern part of the WSB (at 70N/84E and at 65–67N/86–90E) (see summary by Aplonov, 1995).

Presently, Paleozoic crust makes 2/3 of the WSB and includes two major orogenic provinces: the Caledonian block in the south (part of the Proterozoic-Paleozoic Kazakhstan orogenic belt) and the Hercynian block in the central-western parts of the WSB. By Caledonian and Hercynian we refer to deformation events that occurred at ca. 500–400 Ma and 350–300 Ma, respectively.

4.2. Major tectonic events

To simplify further discussion of the crustal structure by tectonic settings and its link to regional geodynamic processes, we summarize briefly the tectonic history of the regions (Figs. 4, 5). A simplified tectonic map of the basement based on a set of geophysical, geological and geochronological studies is presented in Fig. 6. In the present study we follow the widely used Russian Proterozoic stratigraphic scheme, largely constrained by the Siberian stratigraphic sequences (Table 4).

4.2.1. Main Archean–Paleoproterozoic events (3.6–1.7 Ga)

The basement ages of the SC are chiefly Archean (3.25–2.5 Ga), except for the Olenek province in the north-eastern part of the craton (2.4–1.85 Ga) (Rosen et al., 1994). The Paleoproterozoic Akitkan and the Angara orogenic belts are formed by a strongly deformed Archean

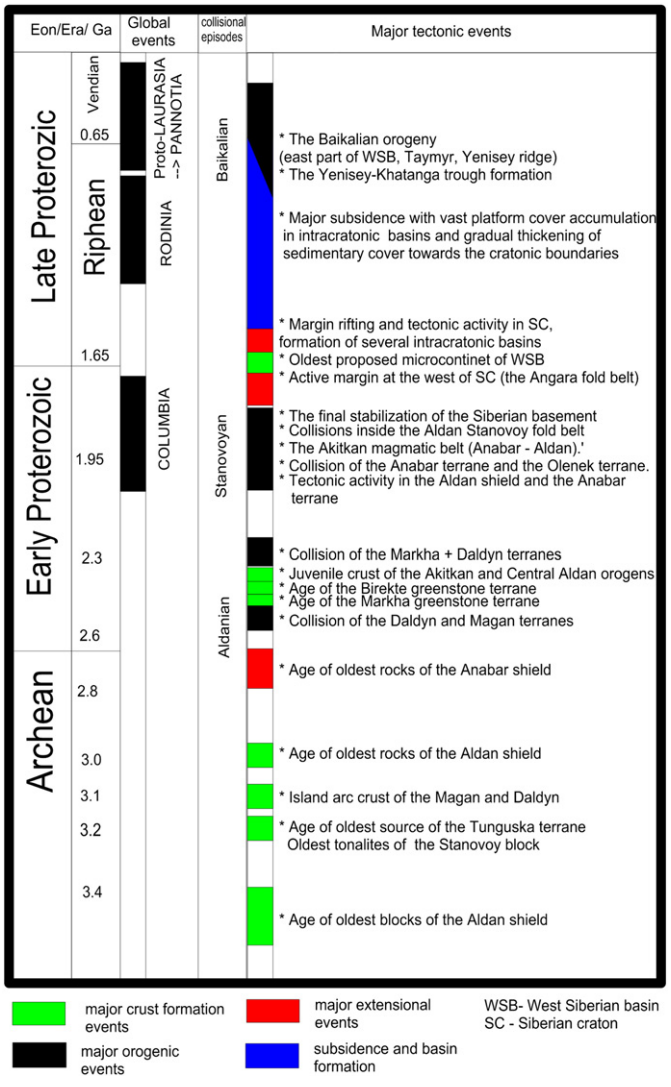

Fig. 4. Summary of the Precambrian tectonic evolution of Siberia.
Data sources: Aplonov, 1995; Bekzhanov et al., 1974; Bradley, 2008; Gladkochub et al., 2006; Jahn et al., 1998; Milanovskiy, 1996; Nikishin et al., 2010); Nutman et al., 1992; Pisarevsky and Natapov, 2003; Rosen, 2003; Rosen et al., 1994; Sklyarov et al., 2001; Surkov and Smirnov, 2003; Vernikovsky et al., 2003; Zhao et al., 2002; Zonenshain et al., 1990.

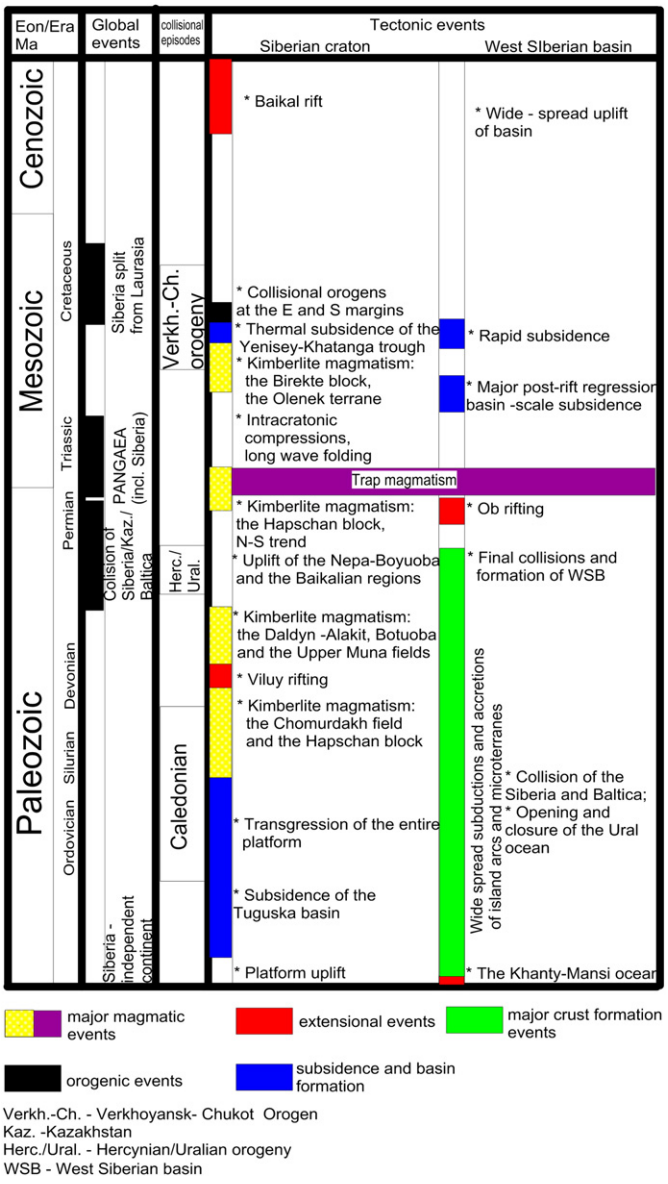

Fig. 5. Summary of the Phanerozoic-Cenozoic tectonic evolution of the Siberian Craton and the West Siberian basin.
Data sources: Al'mukhamedov et al., 1998; Aplonov, 1995; Arkhipov, 1971; Artyushkov and Baer, 1986; Baldin, 2001; Bazanov et al., 1976; Courtillot et al., 2010; Davis et al., 1980; Drachev et al., 1998; Fedorenko et al., 1996; Fokin et al., 2001; Ilupin et al., 1990; Khain, 2001; Klets et al., 2006; Kontorovich et al., 1975; Kushnir, 2006; Logatchev and Zorin, 1987; McKerrow et al., 2000; Metelkin et al., 2007; Milanovskiy, 1996; Nikishin et al., 1996, 2010; Parfenov and Kuzmin, 2001; Pavlov, 1995; Prokopiev et al., 2008; Reichow et al., 2002; Rudkevich, 1974; Sengör et al., 1993; Surkov and Zhero, 1981; Vernikovsky, 1996; Vyssotski et al., 2006; Wooden et al., 1993; Zhuravlev, 1986; Zonenshain et al., 1990; Zorin et al., 2003.

crust and some juvenile Paleoproterozoic crust (Gladkochub et al., 2006). The SC was assembled at ca. 2.6–1.8 Ga by collisions of several Archean and Paleoproterozoic terranes, with related major tectonic and metamorphic events at ca. 2.1–1.8 Ga (Gladkochub et al., 2006; Rosen, 2003). Final stabilization of the SC took place at ca. 1.9–1.8 Ga when large volumes of collisional granites intruded over a significant part of the craton, including the Tunguska province, the Angara fold belt, and the collisional zones between major terranes (Jahn et al., 1998; Nutman et al., 1992; Rosen et al., 1994; Zhao et al., 2002; Zonenshain et al., 1990).

4.2.2. Main Meso- and Neoproterozoic events (1.7–0.65 Ga)

Intracratonic rifting of the Paleoproterozoic protocontinent along the southern margins of Siberia (~1.73–1.68 Ga) (Gladkochub et al., 2006) was followed by rifting both to the east and west of the Anabar Shield (Milanovskiy, 1996). Post-rifting general subsidence of the craton took place at around 1.6 Ga, with an overall thickening of the Riphean successions towards the western side of the craton (Pisarevsky and Natapov, 2003).

The Baikalian orogeny (860–630 Ma) marks the beginning of a common evolution of the SC and the WSB. The Baikalian foldbelt was formed along the western margin of the SC by collision and accretion of terranes, including the Yenisey Ridge island arc and ophiolite belt complex (Vernikovsky et al., 2003). In the north, the collision of the SC with the Taymyr island-arc terrane formed the Taymyr Baikalides. The formation of the deep Yenisey–Khatanga trough began at the same time (Nikishin et al., 2010).

Extensive magmatic activity with widespread mafic dyke swarms (780–740 Ma) affected the southeastern and southern parts of the craton (Gladkochub et al., 2006). Neoproterozoic intracratonic rifting was possibly related to the break-up of Rodinia (Zonenshain et al., 1990). These processes led to rapid Late Riphean subsidence of the craton with the formation of ca. 1–4 km deep basins within the craton

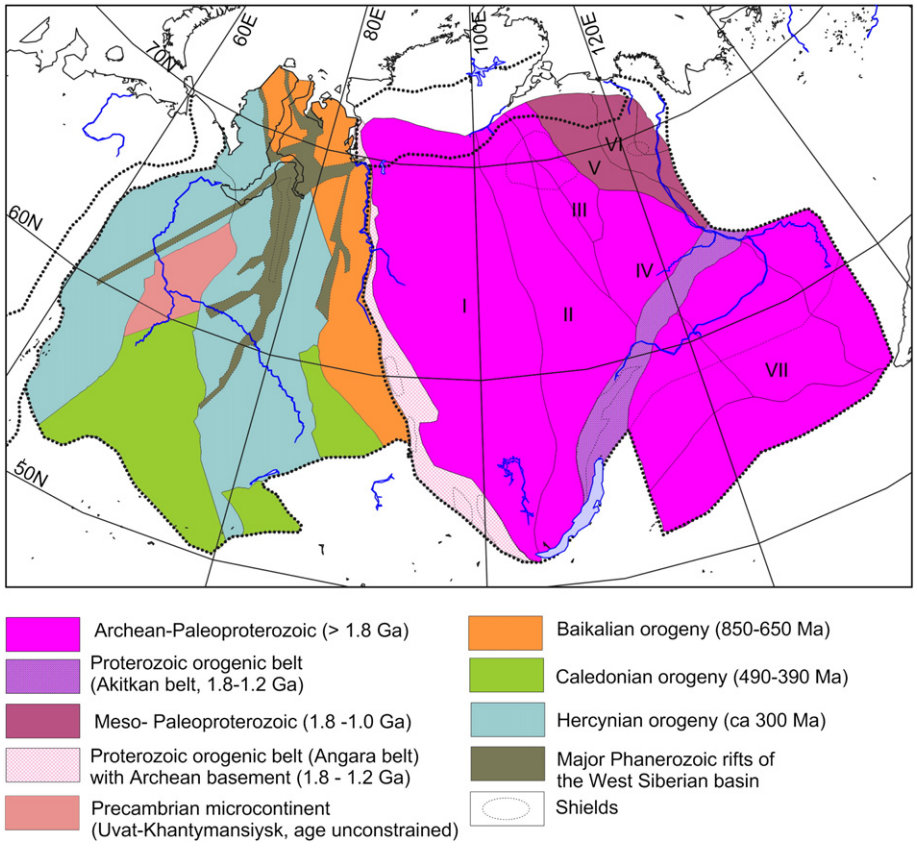

Fig. 6. Tectonic map of Siberia. Bold dotted lines—boundaries of the SC, WSB, and the Urals orogen. Thin black lines—terrane boundaries within the SC. The terranes are: I—Tunguska; II–IV—Anabar superterrane (II—Magan, III—Daldyn, IV—Markha); V–VI—Olenek superterrane (V—Hapchan; VI—Birekte); VII—Aldan–Stanovoy terrane. Basement rocks outcrop mostly in the Anabar and Aldan shields and in the Olenek uplift (the Birekte terrane).
Data sources: Aplonov, 1995; Rosen, 2003; Sengör et al., 1993; Surkov and Smirnov, 2003.

and 10–14 km deep basins along the cratonic margins (Sklyarov et al., 2001). The only major areas that have not experienced the Riphean subsidence are the Aldan–Stanovoy block, the Anabar shield, and the Nepa–Botuoba block. By ca. 650 Ma, the inner parts of the craton were again uplifted above sea level.

4.2.3. Major Vendian–Silurian events (650–400 Ma)

Large-scale subsidence of the entire SC and, in particular, the Tunguska basin, was caused either by the Baikalian orogeny or by a thermal (post-rift) subsidence (Nikishin et al., 2010), although there is no evidence of a rift structure. Formation of passive margins along the northern, western, and eastern margins of the SC resulted in deposition of up to 2 km of salt in the inner parts of the craton (e.g. in the Irkutsk amphitheater) (Khain, 2001; Milanovskiy, 1996).

In the WSB, long-lasting Vendian rifting affected the south-western part of the basin and the area along the Urals. The active rifting ended by the opening of the Khanty–Mansi Ocean between Siberia and Baltica. The Ordovician collision of Siberia and Baltica closed the Khanty–Mansi Ocean and initiated the Ural Ocean (Sengör et al., 1993). Wide spread subduction–accretion orogenic events took place in the south-central part of the WSB.

Table 4
Correspondence between the widely used Russian Proterozoic stratigraphic scheme largely constrained by stratigraphic sequences of the Siberian craton (Semikhatov, 1991) and the International Time Scale (Gradstein et al., 2012).

Siberian stratigraphic scheme	International Time Scale	
Lower Riphean (1.65–1.35 Ga)	Calymmian (1.6–1.4 Ga)	Mesoproterozoic (1.60–1.00 Ga)
Middle Riphean (1.35–1.05 Ga)	Ectasian (1.4–1.2 Ga)	
	Stenian (1.2–1.0 Ga)	
Upper Riphean (1.05–0.65 Ga)	Tonian (1.00–0.85 Ga)	Neoproterozoic (1.00 Ga–542 Ma)
Baikalian (850–630 Ma)	Cryogenian (850–635 Ma)	
Vendian (650–542 Ma)	Ediacaran (635–542 Ma)	

4.2.4. Major Devonian-Permian events (400–250 Ma)

A large-scale Devonian thermal event formed (or reactivated) the 600 km long and wide Viluy rift system in the eastern part of the SC. The rifting was accompanied by substantial mafic and kimberlite magmatism (Courtillot et al., 2010; Parfenov and Kuzmin, 2001), with formation of the West Yakutian diamondiferous kimberlite province at 367–345 Ma at the western end of the Viluy rift (Davis et al., 1980; Ilupin et al., 1990; Rosen et al., 2005). Early-Carboniferous rifting has also affected the Olenek block. Extensive kimberlite magmatism within the SC at 380–240 Ma formed major kimberlite fields, probably along pre-existing lithospheric sutures (Davis et al., 1980; Ilupin et al., 1990).

The southern parts of the Siberian craton were subject to large-scale intraplate deformation, probably in response to the collision of the North China block with Siberia (Nikishin et al., 2010), and caused uplift of the Nepa–Botuoba swell. Significant subsidence of the Tunguska basin in the Early-Middle Carboniferous.

Collisional tectonics at the northern, western and southern margins of the WSB, and at the southern margin of the SC was governed

by large-scale collision between the European, Kazakhstan and Siberian paleocontinents (Khain, 2001). In the north, the Kara terrane collided with the northern margin of the Siberian paleocontinent (Vernikovsky, 1996). In the west, the collisional events formed the Urals (e.g. Fokin et al., 2001; Nikishin et al., 1996). In the south, collision of the WSB with the Precambrian Kazakhstan blocks led to a widespread emplacement of granitic batholiths (280–260 Ma) and to high-grade metamorphism in the south-central part of the WSB (Surkov and Zhero, 1981).

4.2.5. Major Triassic events (250–200 Ma)

Large-scale rifting affected the axial part of the WSB at the initial stage of the Pangaea break-up (Kontorovich et al., 1975; Surkov and Zhero, 1981); it formed a network of sublongitudinal rifts (Pavlov, 1995) and reactivated the Yenisey–Khatanga trough at the northern margin of the SC (Aplonov, 1995). Major basin-scale rapid post-rift compositional and/or thermal subsidence took place in the Jurassic (Artyushkov and Baer, 1986). Flood basalt magmatism (Siberian trap or Siberian LIP) took place in the WSB and the SC at 250 Ma.

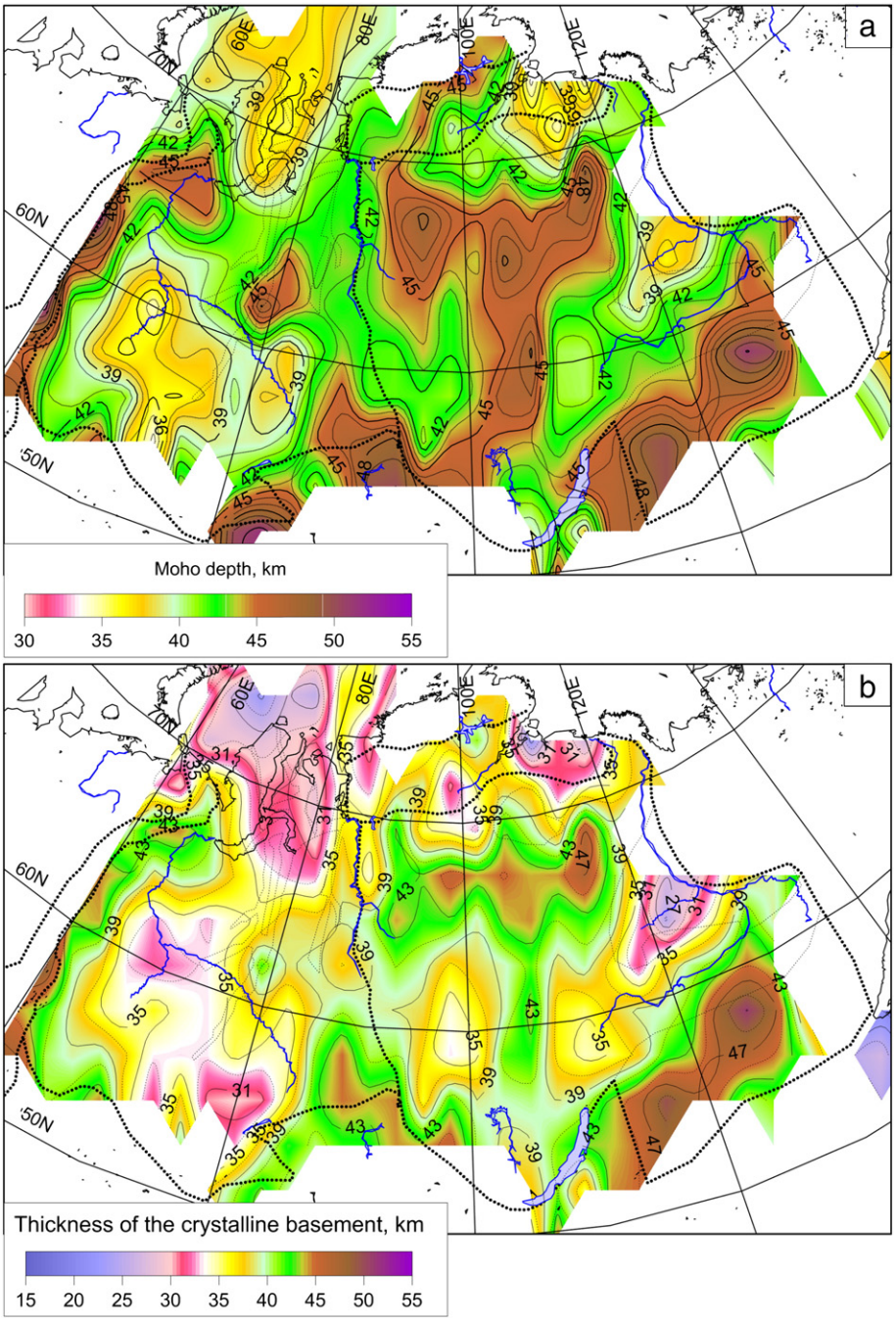

Fig. 7. Maps showing the depth to Moho (a), thickness of the crystalline (consolidated) basement (b), and thickness of sediments (c). The traps and the underlying high-velocity metasediments (Vp > 6.1 km/s) are considered to be a part of the crystalline crust. Map (c) is based only on the profiles listed in Table 3 and does not incorporate existing abundant industrial (but largely inaccessible) borehole data. For this reason map (c) may be less accurate and with a lower resolution than regional maps based on borehole data (in particular for the WSB and the Viluy basin). The map for the thickness of the crystalline basement (b) can be interpreted as showing the difference between the depth to the Moho (a) and thickness of the sediments (c). However, due to the aforementioned limitations of our database for the thickness of sediments, the map (b) was in practice constrained directly from seismic data and independently from the maps (a) and (c). All maps are produced by a nearest neighbor interpolation (chosen to preserve the true amplitudes) with a 2° × 2° interpolation radius (chosen to cover the "white spots", see details in Section 3.4). Information for the Urals is not shown (see maps in Artemieva and Thybo, present volume). Dotted lines—tectonic boundaries (see Figs. 1 and 6).

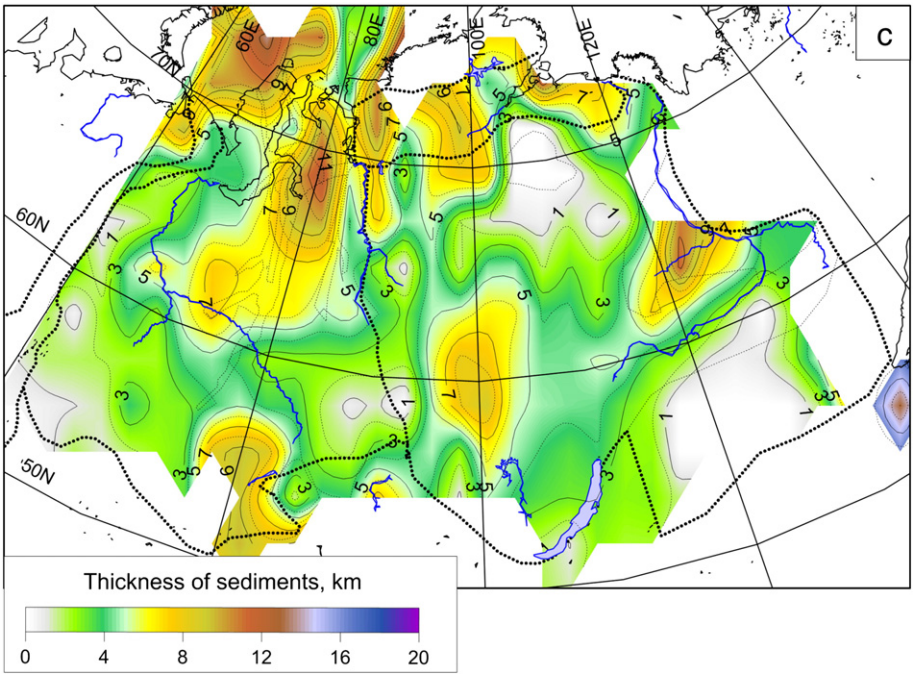

Fig. 7 (*continued*).

The estimates of volcanism duration range from 1 Ma to 50 Ma (Al'mukhamedov et al., 1998). The Siberian traps cover approximately 40% of the Siberian craton with an average lava thickness of ~3500 m (locally >6 km) (e.g. Fedorenko et al., 1996; Wooden et al., 1993) and thinning to a few tens of meters towards the southeast (Vyssotski et al., 2006). A substantial part of the Siberian LIP is buried beneath the West Siberian basin (where basalts are not limited to the major grabens) and the Yenisei–Khatanga trough. The areal extent of basalts beneath the WSB is not well constrained (Reichow et al., 2002; Zhuravlev, 1986). Basalts are also found in the Taimyr Peninsula and may extend beneath the Kara Sea (Vyssotski et al., 2006).

A new pulse of kimberlite magmatism (245–240 Ma) affected the north of the SC along the eastern margin of the Anabar shield. The presence of a belt of alkali-ultramafic intrusions with carbonatites (younger than the Siberian traps) to the west of the Anabar Shield suggests some extensional tectonics, although there is no geological or geophysical evidence for Triassic rifting of the Siberian craton.

4.2.6. Major Jurassic-Cretaceous events (200–65 Ma)

Rapid post-rift subsidence of the WSB took place in the Middle Jurassic with the formation of a few km deep basin. Large scale subsidence of the Yenisey–Khatanga series of basin depressions (Baldin, 2001) led to deposition of Jurassic-Palaeogene sediments with a total thickness ranging from 3 to 5 km in the basins to more than 12 km on the shelf (Kushnir, 2006).

In the SC, rapid post-rift subsidence took place in the Viluy basin. Kimberlite volcanism at 170–140 Ma occurred along a possible Devonian rift at the eastern part of the Olenek terrane (Milanovskiy, 1996). Collisional tectonics shaped the eastern (the Verkhoyansk–Chukchi Orogeny) and southern (the Altai–Sayans orogeny) margins of the SC (Klets et al., 2006; Metelkin et al., 2007; Milanovskiy, 1996; Parfenov and Kuzmin, 2001; Prokopiev et al., 2008; Zonenshain et al., 1990).

4.2.7. Major Cenozoic events (<65 Ma)

The collision of Eurasia with India caused a wide-spread uplift of the WSB as a response to far-field tectonic forces. The Eurasian collision is also responsible, at least in part, for the formation of the Baikal rift at about 30–35 Ma at the suture between the Siberian craton and the Amurian plate (Arkhipov, 1971; Logatchev and Zorin, 1987; Nielsen and Thybo, 2009a,b; Rudkevich, 1974; Thybo and Nielsen, 2009; Zorin et al., 2003). There is no evidence for a recent uplift of the Siberian craton, except perhaps for the Anabar Shield (Bazanov et al., 1976).

5. Results and discussion

Our compilation of crustal seismic models for Siberia forms the basis for the new regional crustal model, SibCrust, illustrated in Figs. 7–13. Based on these maps, crustal cross-sections, and histograms we next describe major features of the crustal structure of Siberia in relation to tectonic setting, from the Archean blocks to Phanerozoic provinces. Rifted crust of the SC and the WSB is discussed separately in Sections 5.3 and 5.5.

5.1. Archean crust

5.1.1. Crustal structure of the Siberian craton

The oldest terranes of the Siberian craton show significant variations in crustal thickness, from 32 to 54 km (Figs. 7a, 9a). The thinnest crust is associated with paleorifts, such as the Viluy rift (see Section 5.3). The thickest crust (>45 km) is observed in three parts of the craton. Two blocks with thick crust correspond to the sublongitudinal suture between the Tunguska and Magan terranes of the SC, and to the Aldan Shield–Stanovoy terrane in the south-eastern part of the craton. The third block includes the area south of the Anabar shield (ca. 65–67° N) with more than 50 km thick crust that extends further westwards into the Tunguska basin. There are no seismic profiles across the central parts of the Anabar shield (Fig. 3), and one cannot exclude that the crust may also be thick there.

A sublatitudinal block of thick Archean crust in the north-central part of the SC (ca. 65–67° N) has a Moho depth of >45 km and locally reaches 54 km (due to the small size of these blocks, they are not well resolved in Fig. 7a). Around the Anabar shield, where the thickness of sediments does not exceed 1–3 km (Fig. 7c), the consolidated basement is generally thicker than 40–45 km (Fig. 7b). Many other parts of the SC where the Moho depth is close to the global average, 40–44 km, have experienced crustal extension and/or thermal subsidence in Proterozoic-Paleozoic time.

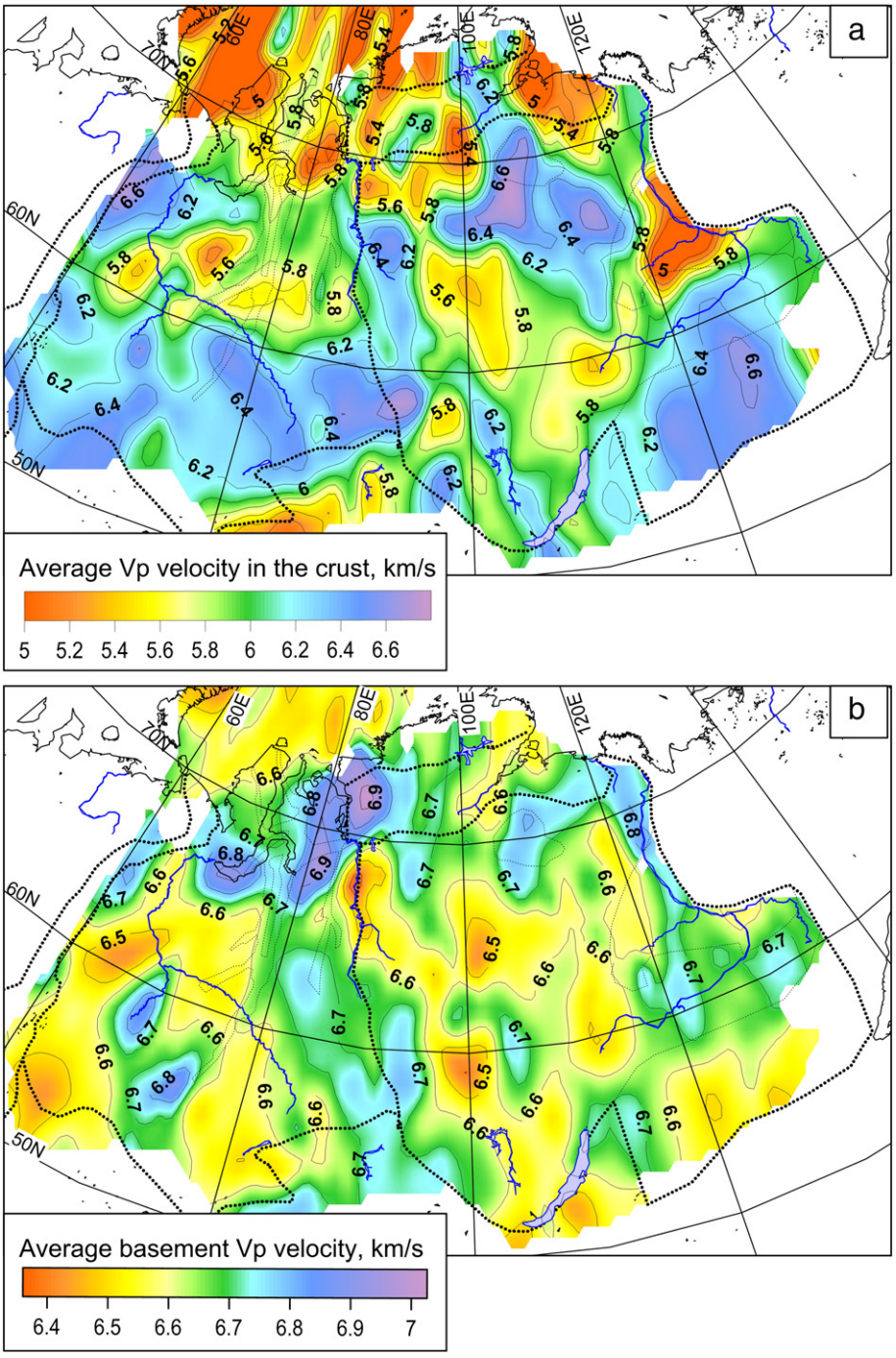

Fig. 8. Maps showing the average Vp seismic velocity in the entire crust (a) and in the crystalline basement only (b). Small-scale "bull's-eye" features are true anomalies observed in the seismic models. Average velocities are calculated by averaging travel times (not Vp) in the individual crustal layers, as $Vp(\text{aver}) = \sum(h_i) / \sum(h_i / V_i)$, where h_i is thickness of individual crustal layers and V_i is Vp velocity in these layers. For interpolation details see caption of Fig. 7. A block with exceptionally high basement Vp velocities (6.8–7.0 km/s) at around 80E/70N can be related to the source zone of the Siberian traps.

The thickness of sediments in the SC varies from near-zero values in areas of exposed basement (the Anabar shield and the Aldan shield) through 3–4 km in most of the inner parts of the craton, to extreme values of more than 15 km in the axial part of the Viluy rift. Note that the map of thickness of sediments (Fig. 7c) is constrained only by published seismic models along the crustal-scale profiles, whereas shallow industrial seismic models are unavailable to the authors. For this reason, the map cannot be used as a high resolution constraint; we estimate the general accuracy to be ca. 1–2 km, but with larger local uncertainty.

The Tunguska basin is covered by a thick basalt sequence of the Triassic traps which overlies older sediments and, in some places, is covered by younger sediments. Note that in the SibCrust model, which is based on seismic velocity information, the traps and the underlying high-velocity metasediments (Vp > 6.1 km/s) are considered to be a part of the crystalline crust, given that the boundary P-wave velocity between the sediments and the basement rocks is adopted as 5.8 km/s. For this reason, thickness of sediments in the Tunguska basin incorporated into the SibCrust model is different from the values based on geological sections (e.g. Nikishin et al.

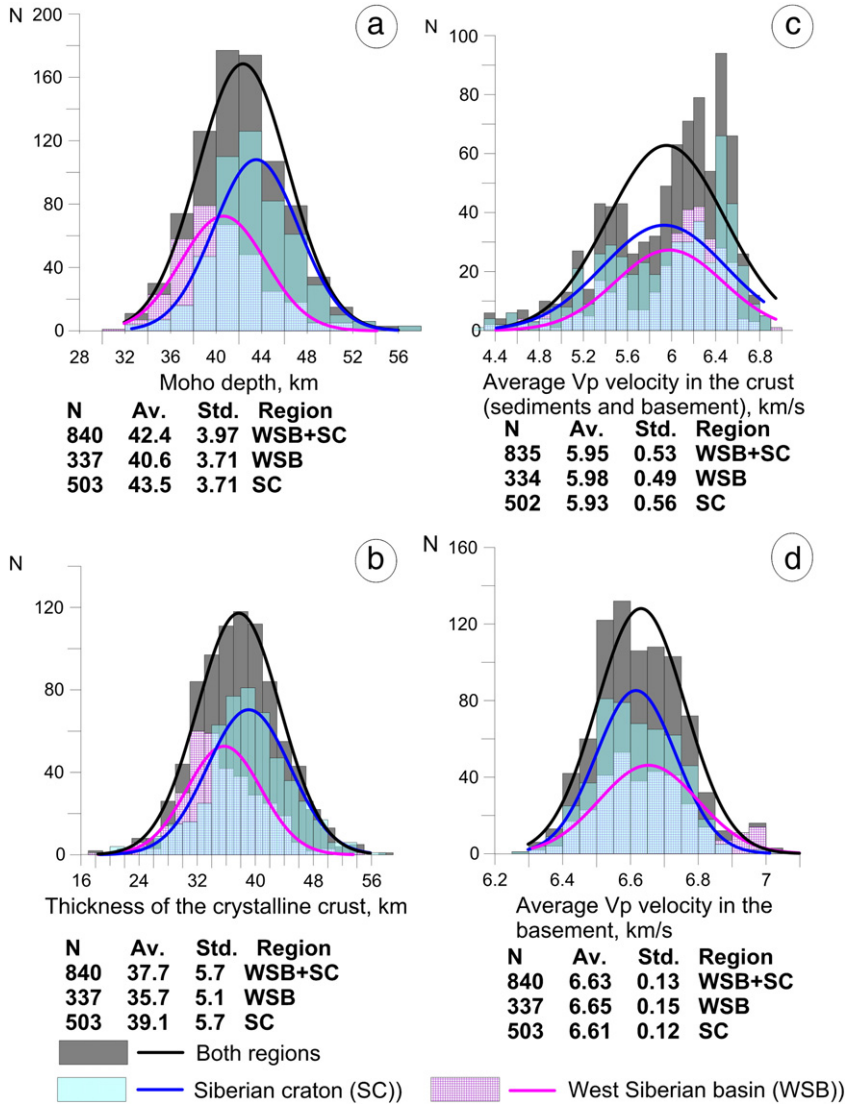

Fig. 9. Histograms for variations in the depth to Moho (a), thicknesses of the crystalline basement (b), average Vp seismic velocity in the entire crust (c) and in the crystalline basement only (d). Regions north of 72N are excluded. Thick lines—best fitting Gaussian distributions. Vertical axes—number of the corresponding entries in the database, based on the point data digitized along the seismic profiles. For details on the digitizing strategy see Section 3.1. Note that statistics may be biased by locations of seismic profiles.

(2010) report a ca. 8 km thickness of the Vendian-early Carboniferous deposits in the Tunguska basin). Besides, it also results in a large thickness of the upper crust (ca. 15 km) in the Tunguska basin (Fig. 10a).

Although, on the whole, the entire crustal structure of the SC is highly heterogeneous, the Archean-Paleoproterozoic crust has a three-layer structure typical of stable continents (Meissner, 1986) with an approximately equal thicknesses of the three layers. Typical thicknesses of the upper (UC), middle (MC), and lower crust (LC) are ca. 15 km, 15–20 km, and 10–20 km, respectively (Figs. 10–12). The conclusion that the Archean crust is thinner than the Proterozoic crust because it has a reduced thickness of (or even lacks) a high-velocity lower crustal layer (Durrheim and Mooney, 1991) is not supported by seismic models for the Siberian craton, since the crust is thick and the lower crust beneath the Archean terranes of the Siberian craton is present everywhere as a 10–20 km thick layer. Furthermore, substantial parts of the Archean crust in Siberia include a high-velocity lowermost crust LMC (Vp > 7.2 km/s) (see profile BB′ in Fig. 12).

As an example, we discuss the structure of the crust in the Tunguska basin. By crustal structure, the Tunguska basin can be divided into two domains with Moho depths of 45–50 km in the north and ca. 40–45 km in the south. The thickness of the sedimentary cover, in contrast, increases from north to south. As a result, in the north the thickness of the crystalline basement exceeds 40 km and the crust has average velocity of >6.3 km/s, whereas in the southern domain the basement is thinner (ca. 35–40 km) and the average crustal velocity is low (6.0–6.3 km/s) (compare Figs. 7c and 8a). The middle crust is the thickest in the north-central parts of the Tunguska basin, locally reaching ca. 20 km in thickness, whereas in the southern parts it generally thins to 5–10 km (Fig. 10a). The central-axial part of the basin (in the area filled by Triassic trap basalts) is underlain by a high-velocity LMC (Fig. 10d) and a high-velocity upper mantle with a Pn velocity of 8.3–8.5 km/s (Fig. 13). It is unclear if this anomaly can be related to a speculative Riphean rift that extends from the northernmost part of the Nepa–Botuoba swell towards the Viluy rift (Sokolov, 1989) and spatially correlates with the region with high Pn velocities.

Within the SC, a high-velocity LMC is also observed at the Proterozoic suture zones of the Anabar province (including the areas of the Devonian kimberlite fields) (Fig. 10d). Given the spatial correlation of the LMC layer with areas affected by Proterozoic-to-Paleozoic magmatism, we speculate that the high-velocity layer at the base of the crust could have been formed by magmatic underplating and its

age may be at least a few hundred millions years old (e.g. Clowes et al., 2002; Korsman et al., 1999; Thybo and Artemieva, 2013–this volume). Except for the rifted crust of the Viluy basin and the Yenisey–Khatanga trough, regions where the LMC layer is present have a thick crust (Fig. 7a). Physical conditions favorable for the preservation of a thick crust without being delaminated are probably provided by very low crustal temperatures as reflected in extremely low heat flow in much of this region, 18–25 mW/m^2 (Artemieva and Mooney, 2001; Duchkov et al., 1987) which impede the metamorphic reaction from basalt to eclogite phase. Although the true rate of this reaction at low crustal temperatures typical for cratons and, in particular, at dry conditions, is unknown (Artyushkov, 1993), it is likely that a cold and dry basaltic layer may remain metastable for geologically long time (Artemieva and Meissner, 2012).

Crustal blocks of the SC with thick crust have, as a rule, high average crustal velocity (Fig. 8a). In particular, it exceeds 6.5 km/s in the

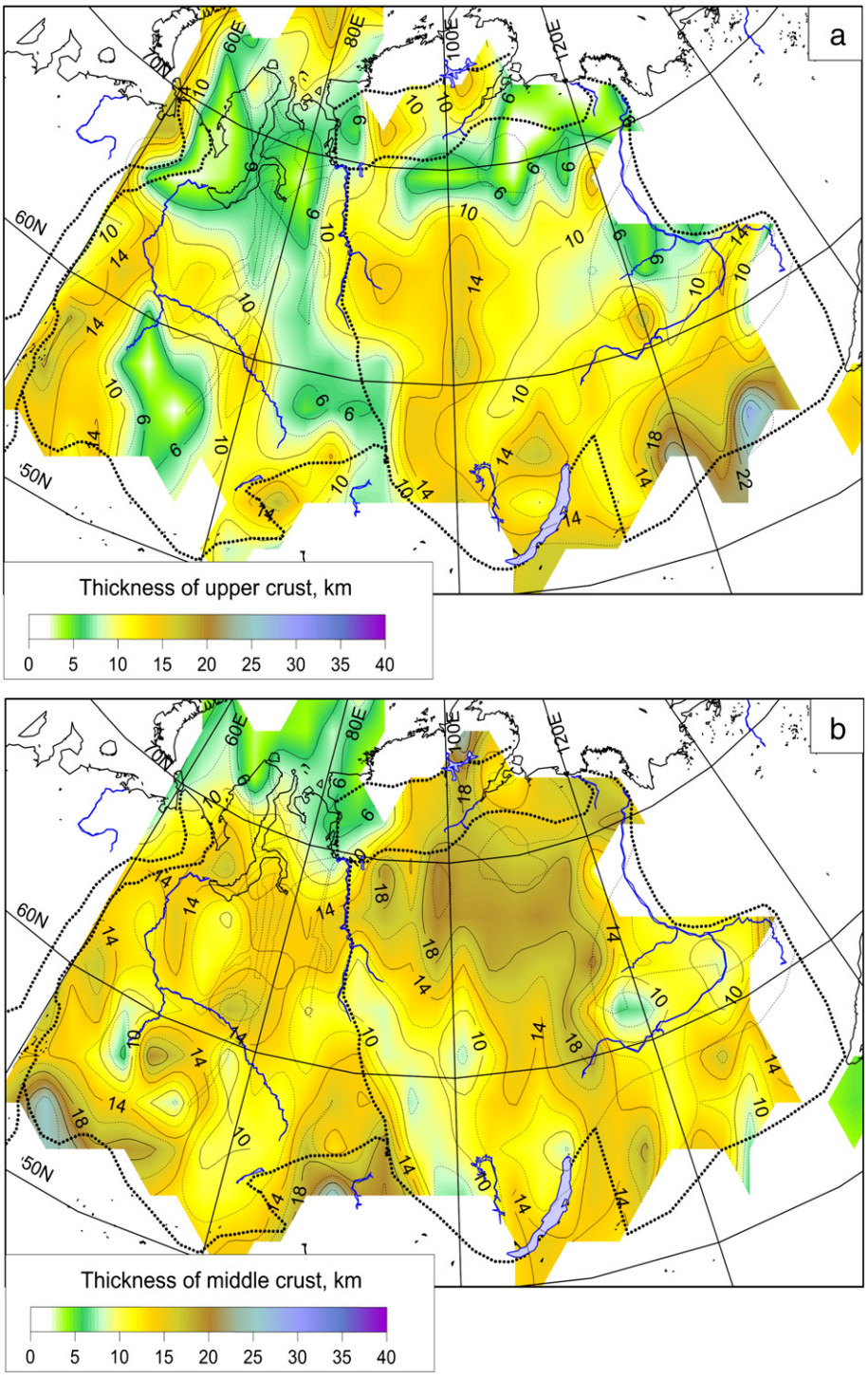

Fig. 10. Thickness of crustal layers as defined by Vp velocities: (a) the upper crust (5.8 < Vp < 6.4 km/s), (b) the middle crust (6.4 < Vp < 6.8 km/s), (c) the lower crust (6.8 < Vp < 7.8 km/s), (d) the lowermost crust (7.2 < Vp < 7.8 km/s) (regions where the lowermost crust is absent are shaded gray; regions not covered by seismic data are left white). The traps and the underlying high-velocity metasediments (Vp > 6.1 km/s) are considered to be a part of the upper crust. In cases where seismic reflectors are observed from refraction-wide-angle reflection surveys, we adopted the crustal layers as identified in the original studies regardless of Vp velocity values in the layers. For interpolation details see caption to Fig. 7.

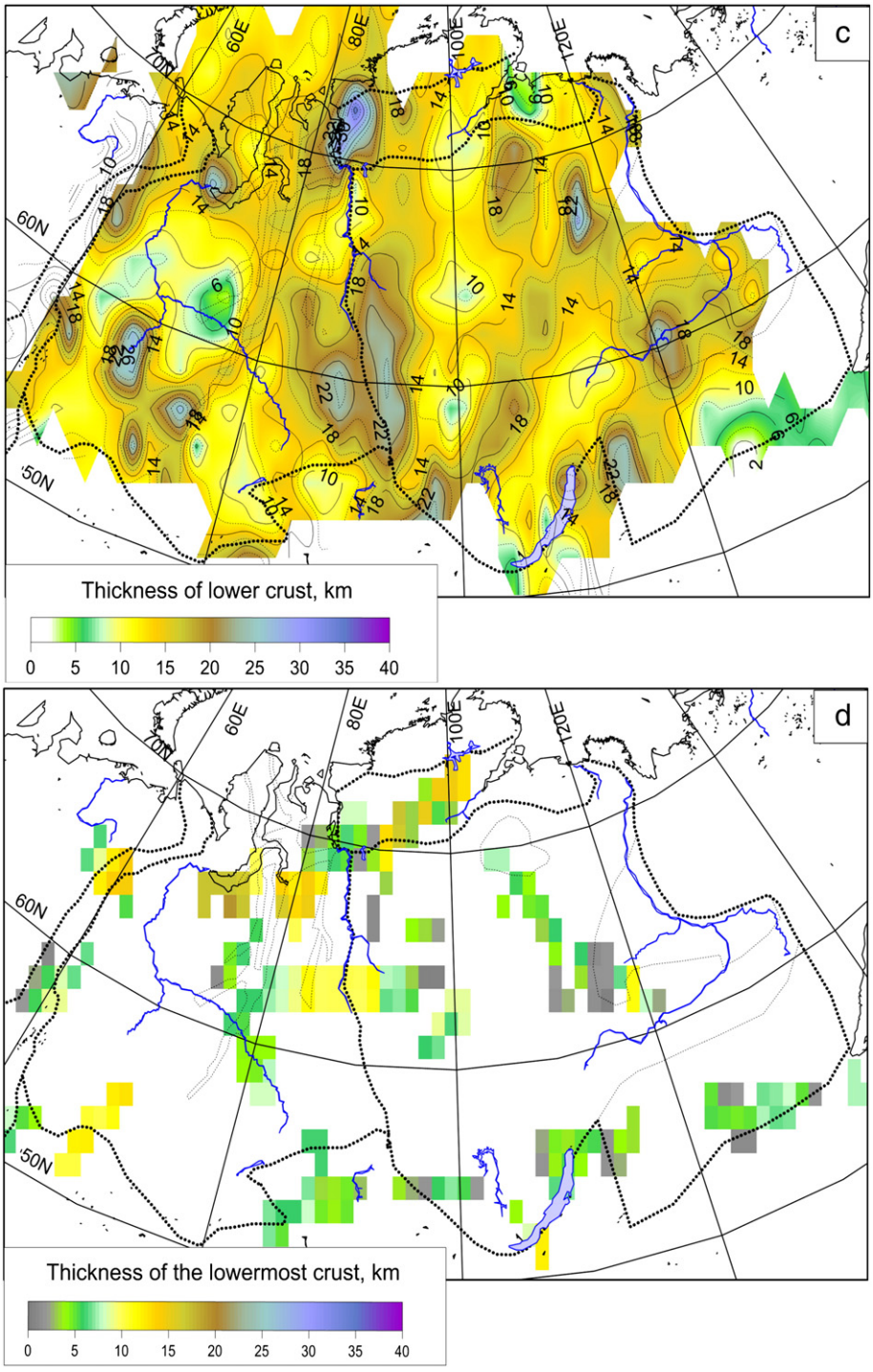

Fig. 10 (*continued*).

Anabar shield and around it, and in the Aldan–Stanovoy terrane. Because of the presence of a thick lower crust in the Anabar province, this crustal block has some of the highest average basement Vp velocities in the SC, 6.7–6.8 km/s (Fig. 8b). Note that only two seismic profiles cross the marginal parts of the Anabar shield and thus seismic information on its crustal structure remains incomplete.

5.1.2. Upper mantle Pn velocity in the Siberian craton

The velocity structure of the upper mantle in the Archean terranes of Siberia is very heterogeneous with Pn values ranging from 7.9 to 8.8 km/s (Fig. 13). Both the extremely low and high velocities are unusual for the Archaean cratons. The worldwide average Pn velocity for the shields and stable platforms is 8.13 km/s ± 0.19, whereas values as low as 7.9–8.0 are typical of extended continental crust and rifts (Christensen and Mooney, 1995). Relatively low Pn values (<8.05 km/s) are observed at the eastern part of the Yenisey–Khatanga trough as well as around the major Paleozoic kimberlite fields, next to extremely high values of 8.7–8.8 km/s observed in the same area (Suvorov et al., 2006). Since the global crustal models CRUST 5.1 and CRUST 2.0 assign a constant Pn velocity value of 8.2 km/s to the upper

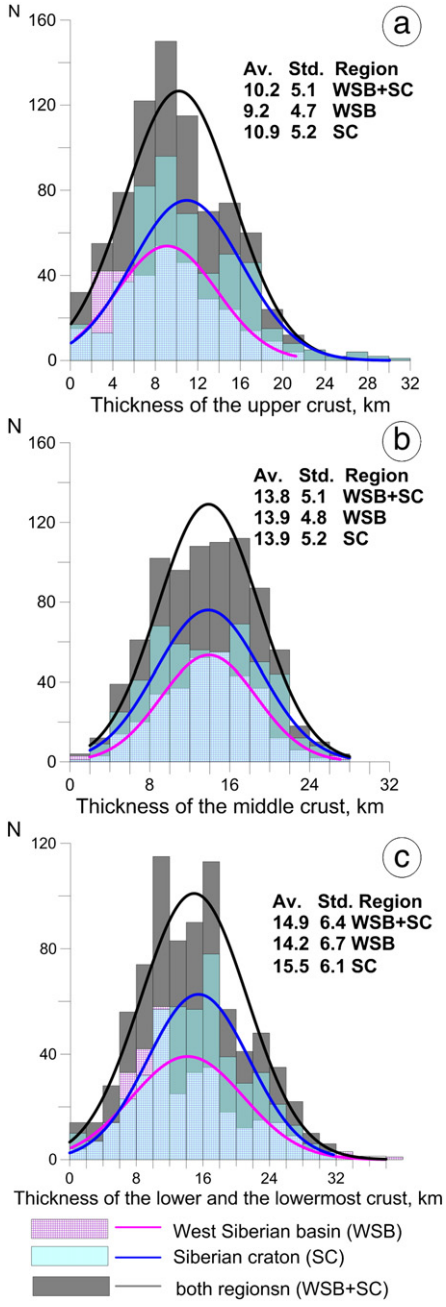

Fig. 11. Histograms for variations in the thicknesses of the upper (a), middle (b), and lower (c) (Vp > 6.8 km/s) crust based on the point data digitized along the seismic profiles. For details see caption of Fig. 9. Note that statistics may be biased by locations of seismic profiles.

mantle of entire Siberia (both the WSB and the SC), the difference between the true seismic Pn velocity and the value adopted in the global crustal models ranges from −0.3 to +0.6 km/s (Fig. 14b).

The Siberian craton is unique in having the highest reported Pn velocities of up to 8.8–8.9 km/s around kimberlite fields (Nielsen et al., 1999; Suvorov, 1993; Suvorov et al., 2006; Uarov, 1981) and 8.5 km/s in the axial zone of the Tunguska basin and within the Viluy basin (Pavlenkova et al., 2002). Until recently, based on the early seismic studies, it was thought that these extremely high velocity values are characteristic of the whole area around the Siberian kimberlite fields. Recent high-resolution seismic studies demonstrate that they appear only in 100 km to >300 km wide segments intersected by regions with normal Pn velocity of 8.1–8.2 km/s (Suvorov et al., 2006). The extremely high P-velocity values interpreted in seismic models have not been reported from laboratory measurements on peridotites and therefore, they were for long considered either erroneous or caused by strong (extreme) anisotropy in the subcrustal mantle. However, regional seismic data do not provide conclusive evidence for a significant azimuthal anisotropy in the Siberian craton, despite that the anomalous high Pn has been observed at different azimuths (Nielsen et al., 2002; Pavlenkova, 1996; Suvorov et al., 1999). Note that this indication does not fully exclude anisotropy as the cause (Suvorov et al., 2006) and recent laboratory studies of Siberian peridotites indicate that a significant upper mantle anisotropy is possible in the Siberian upper mantle (Bascou et al., 2011; Kobussen et al., 2006).

Laboratory measurements of seismic velocity have, so far, been carried out only on three peridotite and two eclogitic mantle rocks from the kimberlite province (Kobussen et al., 2006). The maximum measured Pn velocity is 8.6 km/s which is less than the highest velocities reported in seismic models (8.8–8.9 km/s). These authors also calculate the theoretical velocities based on the measured mineral composition, grain size and crystal orientation in the samples, by which they find that velocities as high as 9.1 km/s are possible in dunites at the required temperature and pressure conditions. A recent laboratory study by Bascou et al. (2011) of the composition and grain size distribution in mantle xenoliths from the Udachnaya kimberlite pipe (the Daldyn terrane) leads to a similar conclusion. These authors suggest that coarse peridotites have much higher anisotropy than eclogites, in agreement with seismic data from other settings (Wang et al., 2005), and may yield high (Vp ≥ 8.8 km/s) P-wave velocities in the fast direction. Thus, both experimental studies on rock samples from the Siberian kimberlite province provide indication that the extremely high sub-Moho velocities (Vp > 8.7 km/s) reported from several seismic profiles in the Siberian craton may be better explained by strong anisotropy of coarse peridotites in a horizontally foliated mantle than by the presence of abundant eclogites. In particular, dunites and spinel harzburgites are proposed as the best candidates to explain the extremely large P-wave velocities in the sub-Moho mantle in the kimberlite fields of the Siberian craton (Bascou et al., 2011; Kobussen et al., 2006). However, it still remains to directly measure such extreme velocities in the laboratory.

5.1.3. Comparison with other cratons and global crustal models

The new regional crustal model indicates that the Archean crust in Siberia is strongly heterogeneous and, in general, much thicker than the global average for the cratonic crust (40–42 km, Mooney et al., 1998). Similar observations are not unique for Siberia and have been reported for the Archean crust of the Canadian Shield, India, and Southern Africa. Recent seismic studies in the Kalahari craton based on the high-resolution SASE data demonstrate that the structure of the crust is strongly heterogeneous with the Moho depth changing over short distances from 31–34 km to 53–57 km (de Wit and Stankiewicz, 2013–this volume; Kwadiba et al., 2003; Nair et al., 2006; Nguuri et al., 2001; Nui and James, 2002; Youssof et al., 2012, 2013–this volume). In contrast, the pre-2000 seismic models indicated a relatively thin (ca. 37 km) and uniform crust in the Kaapvaal craton (e.g. de Wit et al., 1992; Durrheim and Mooney, 1991). Thin crust (30–35 km) is, however, typical for the oldest portions of the West Australian craton, the Pilbara craton and the northern Yilgarn craton (Kennett et al., 2011; Salmon et al., 2013–this volume).

It is worth mentioning that the seismic database that forms the basis for global statistics on the crustal structure for the Archean-Paleoproterozoic regions (Mooney et al., 1998), and therefore for the global models CRUST 5.1 and CRUST 2.0, has been significantly biased by an overweight of available crustal models for Southern Africa and Western Australia reported in the pre-2000 studies, while these models may be non-representative globally or even regionally as in the case of the Kaapvaal. This results in significant differences in the depth to Moho and other crustal parameters between the true crustal structure in Siberia and the global crustal models due to the

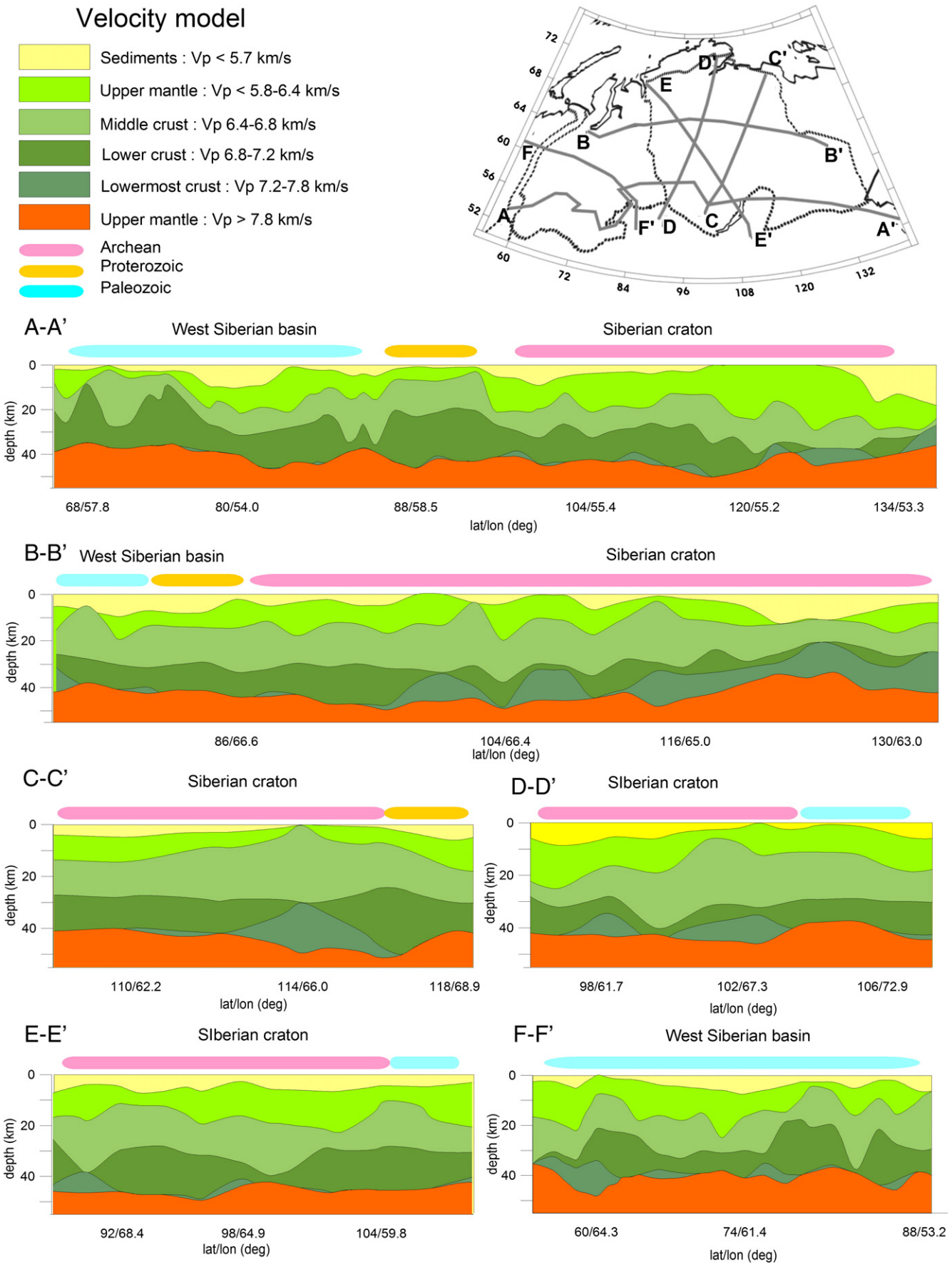

Fig. 12. Crustal cross-sections based on the new crustal model SibCrust. The locations are chosen to cross the major tectonic structures which are well covered by high-quality seismic data. Vertical and horizontal dimensions are not to scale.

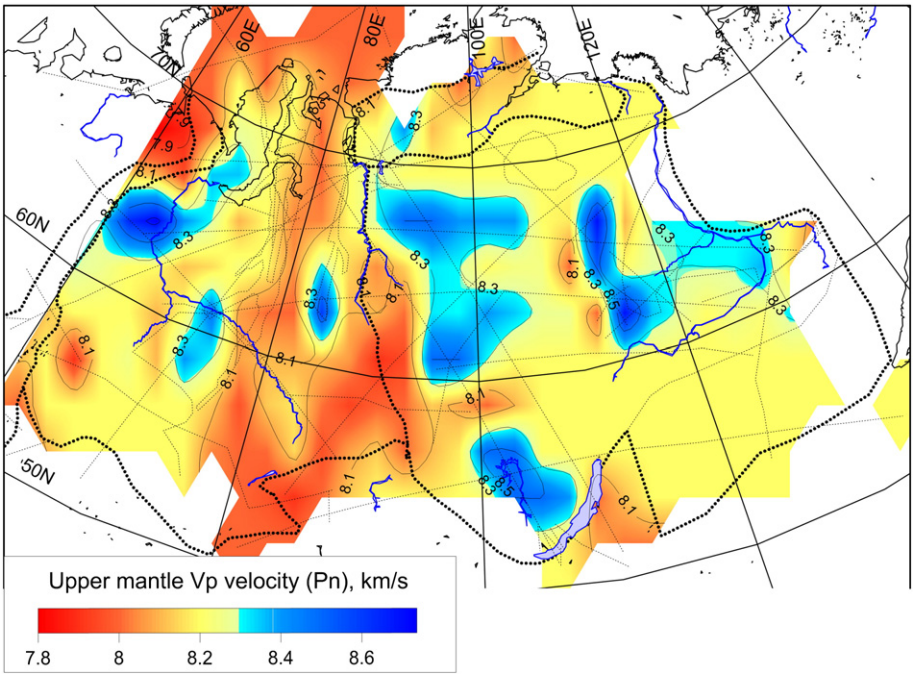

Fig. 13. Maps showing the upper mantle Pn velocities. Small-scale "bull's-eye" features represent true anomalies observed in the seismic models. For interpolation details see caption to Fig. 7.

assignment of parameters by tectonic analogy (Fig. 14a). Specifically, the true average Vp velocity in the crystalline basement is 0.2–0.3 km/s higher than in the CRUST 5.1 and CRUST 2.0 models almost everywhere in Siberia (both in the WSB and the SC), with an extreme difference of ca. 0.4–0.6 km/s in the Tunguska basin and the northern part of the WSB.

The Siberian craton is not the only Archean terrane with deep Moho and thick lower crust. Thick crust has also been reported for the Archean West Dharwar craton in southern India, where the crustal thickness varies between 42 km and 60 km; the latter value is observed beneath an exhumed granulite terrane, while a thickness of 50 km is reported for the mid-Archean greenstone belt in the craton nucleus that has not been subject to any severe compressive deformation (Mall et al., 2012). Similar to the Siberian craton, the region with thick Archean crust in India is characterized by low surface heat flow (31 ± 4 mW/m^2) (Gupta et al., 2003; Roy and Mareschal, 2011; Roy and Rao, 2003) and high lower crustal (7.4 km/s) and upper mantle Pn velocities (8.35 km/s) (Mall et al., 2012). Likewise, the presence of a thick crust (around 60 km thick) has been reported for the Archean-Proterozoic suture of the Baltic shield at the boundary between the Kola–Karelian and the Svecofennian provinces (Korja et al., 1993) in a region with low heat flow (Kukkonen, 1998). In the Canadian Shield, the 800 km long Lithoprobe's SAREX profile from east-central Alberta to central Montana revealed the presence of a 10–25 km thick lower crustal layer with high velocities (7.5–7.9 km/s) beneath the Archean Medicine Hat and Wyoming blocks (e.g. Clowes et al., 2002). Crustal blocks with the thickest lower crust, interpreted as magmatic underplating caused by Paleoproterozoic tectonic events (for discussion see Thybo and Artemieva, present volume), correspond to the thickest crust where the depth to Moho is up to 60 km.

5.2. Paleoproterozoic crust

Paleoproterozoic crust forms the Olenek terrane at the northeastern corner of the Siberian craton (Fig. 6). The principal suture zones between the Archean domains of the SC also have Proterozoic age; they include Proterozoic granites without evidence for the presence of juvenile crust. On the other hand, juvenile Paleoproterozoic crust of island arc origin is well-documented for the Akitkan magmatic fold belt. Paleoproterozoic crust also marks the western margin of the SC, where it outcrops in the Yenisey Ridge.

The Olenek terrane, especially its southern part, is poorly covered by seismic profiles (Fig. 3). The available seismic models indicate the Moho depth of ca. 43 km decreasing northwards into the extensional crust of the Lena–Anabar trough with a thick sedimentary cover (Fig. 7). The thickness of the upper crust increases from <5 km in the north to 10–15 km in the south; the latter may be its original, Proterozoic, thickness. The extended crust in the northeast has a thick (15 km) middle crust, 3–5 km thinner than the MC in the adjacent Archean Anabar block. Beneath the Berikte granite-greenstone massif, that forms the central block of the Olenek terrane, the thickness of the lower crust is 10–15 km and increases to 15–20 km beneath the Khapchan belt in the west and beneath the northeastern part of the Olenek High. Locally, at the suture zones between the Archean and Archean-Proterozoic blocks, the lower crustal thickness increases to 20–25 km (Fig. 10). No high velocity LMC is observed in the Paleoproterozoic crust of the Olenek province (profile CC′ in Fig. 12), and the Pn velocity is normal, 8.1–8.2 km/s, slightly lower (8.1 km/s) northwards in the extended crust (Fig. 13).

The Moho depth around the craton-scale Proterozoic sutures is not uniform and varies from 40 km in the northern parts of the craton near the Yenisey–Khatanga trough to 54 km at two major suture zones, where the deepest Moho in the Paleoproterozoic parts of the studied region is reported. The latter include the central part of the Billyah collision suture between the Anabar and the Olenek provinces (with an anomalously thick LC, 31 km) and the suture between the Archean Daldyn granulite terrane and the Archean Markha granite–greenstone terrane.

The crustal structure of the Paleoproterozoic Akitkan magmatic collisional belt (Fig. 6) has been significantly modified by Devonian extensional tectonics and the associated magmatism in the Vilyu rift, and possibly earlier by proposed Neoproterozoic rifting events. The Moho depth is ca. 40 to 44 km and is significantly more shallow than beneath the adjacent terranes (Fig. 7a). The Akitkan belt is clearly marked by a sharp change in the thickness of the upper crust, which thins in a step-wise manner from 15 km in the adjacent terranes to 10 km in the Akitkan belt (Fig. 10a). Similar to other

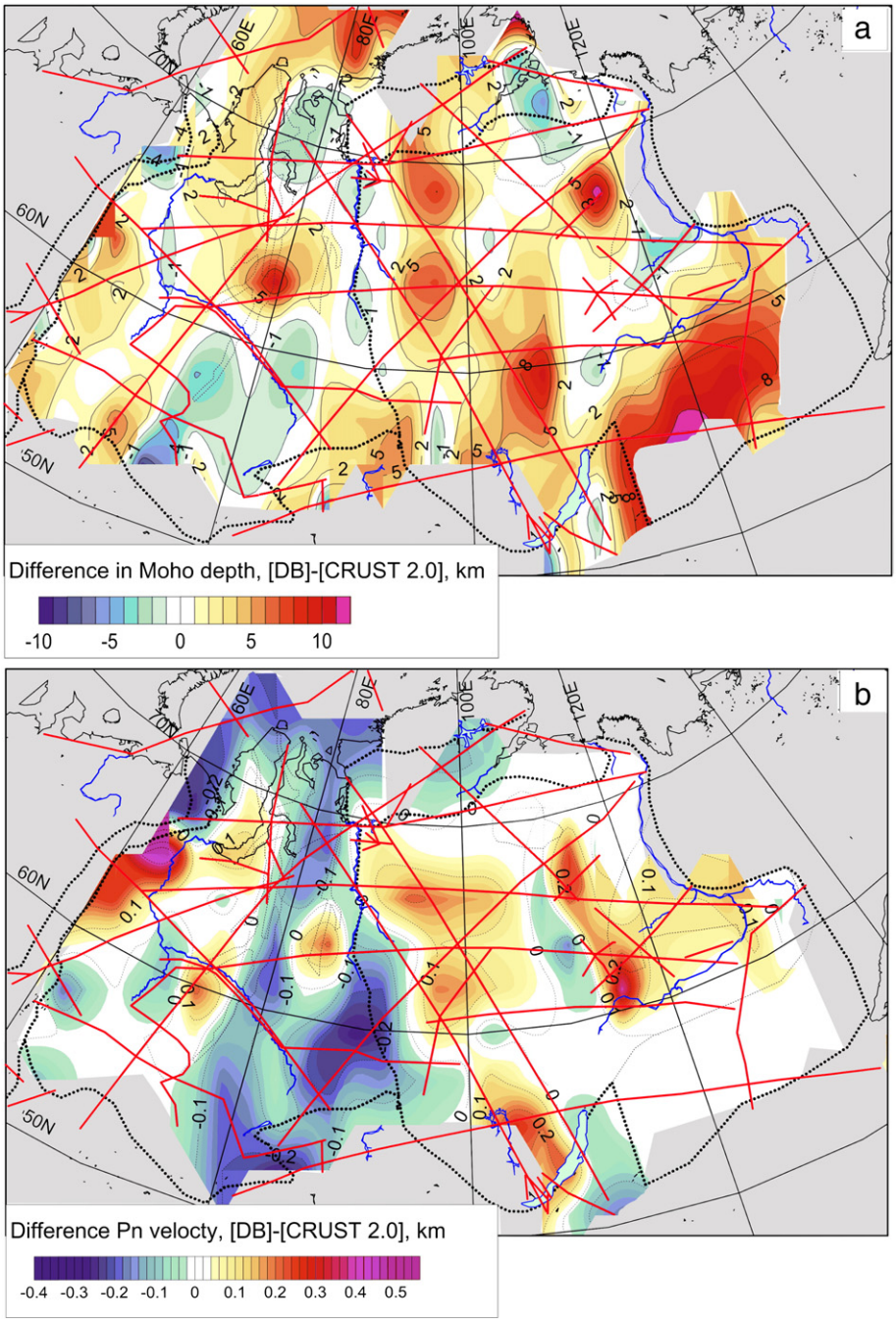

Fig. 14. Map illustrating the differences between the new crustal model SibCrust and the CRUST 2.0 model (Bassin et al., 2000) for (a) the Moho depth and (b) the Pn velocity. Both crustal models are constrained by a 2° × 2° nearest neighbor interpolation with the same interpolation parameters. Regions not covered by the SibCrust model are not compared and are shown by gray color.

Paleoproterozoic blocks, no LMC is observed in the belt, except for a local anomaly probably associated with the Viluy rift.

The crustal structure of the Yenisey Ridge is similar to the Akitkan belt. The crustal thickness is 40–45 km, with a significantly thinned upper and, particularly, middle crustal layers (5–10 km) which is in a strong contrast to the adjacent crustal blocks of the Siberian craton and the Baikalian foldbelt. In contrast, the lower crust in the entire Yenisey Ridge and the adjacent areas is 20–25 km thick, but lacks a high-velocity LMC. The average basement velocity is ca. 6.8 km/s which is in contrast to the crust of the adjacent Tunguska basin (<6.6 km/s). These crustal features are associated with the presence of island arc and ophiolite complexes in the Yenisey Ridge.

On the whole, the Paleoproterozoic crust of the SC has a highly variable crustal thickness ranging between ca. 40 km and >50 km (Fig. 7). In comparison to the Archean crust of the SC, the sedimentary cover is much thicker, both UC and MC are thinner, the LC is usually thicker, but no LMC is present (Figs. 10, 12), and the Pn values are similar to many other stable continental regions worldwide (8.0–8.2 km/s) (Fig. 13).

The presence of several buried Precambrian blocks under the sedimentary cover of the WSB has been proposed based on potential field studies (e.g. Aplonov, 1995; Bekzhanov et al., 1974). The largest proposed block, the (Meso-) Proterozoic Uvat–Khantymansiysk median massif, is crossed by several high-quality seismic profiles (Fig. 3).

For this block, seismic models indicate a crustal thickness of 35–40 km, 3–8 km of sediments, thick (10–15 km) upper crust, thin (>10 km) lower crust, absence of the fast LMC layer, and as a consequence a pronounced minima in the average Vp velocity (6.4–6.5 km/s) and the thickness (ca. 32 km) of the crystalline crust (Fig. 7b).

5.3. Rifted crust of the Viluy basin

The central part of the Devonian Viluy rift system (located along the Proterozoic Akitkan magmatic belt) is formed by two major branches (the Kempendyai and the Markha grabens) filled with 5 to 14 km alkaline basalts and sedimentary rocks; radially-arranged mafic to ultramafic dyke swarms are widely present at its periphery (Parfenov and Kuzmin, 2001). The thickness of the crystalline crust beneath the axial part of the Viluy rift is 16–32 km, with the Moho at 35 km depth in the axial part of the rift system, increasing to 45 km depth in the peripheral parts. The UC is the thinnest (0–5 km) and the Moho is the shallowest in the eastern part of the rift. Thin upper crust follows two major branches of the rift, which are separated by a block with 10–15 km thick UC. Local thickening of the UC to 20 km (coincident with thinning of the middle crust to almost zero) is observed between the two major rift branches near their junction. There is no further correlation between the inner structure of the crust and the rift branches. The MC is ~10 km thick and LMS is thick (up to 10 km) beneath most of the rift, which may be related to underplating. The average Vp velocity in the crystalline basement of the Viluy basin is locally ca. 6.7–6.8 km/s and is higher than in most of the SC (except for the Anabar block region) (Fig. 8b). Pn velocities beneath the Viluy basin are high (up to 8.3–8.4 km/s) and are similar to those beneath the Tunguska basin.

5.4. Baikalian, Caledonian, and Hercynian fold belts of the WSB

Neoproterozoic crust (mostly formed during the Baikalian orogeny, ca. 850–650 Ma) forms the narrow belt between the WSB and the SC. The crustal structure is better known in the northern part which is crossed by several seismic profiles (Fig. 3). Crustal thickness in the Siberian Neoproterozoic crust varies between 33 and 45 km, with thin crust (33–40 km) in the extended Pur–Taz basin in the north and thick crust in the south (Fig. 7a). Crustal thickness decreases from ca. 35 km in the onshore Arctic part of the Baikalian belt to 28–30 km towards the offshore area. Thickness of the sedimentary cover is 0–3 km in the south and 6–16 km thick in the north. The upper crust of the Baikalian fold belt is usually thin (5–10 km, and almost absent in the Pur–Taz basin), whereas the lower crust is thick (>20 km in some crustal blocks), and the presence of high-velocity lowermost crust is common (Fig. 10). For example, in the Pur–Taz basin the lowermost crust has velocity of 7.4–7.6 km/s and is 8–16 km thick. As a result, the Baikalian belt is marked by high average basement velocities (6.7–6.8 km/s), which are similar and only slightly lower than in the Yenisey Ridge (Fig. 8b). The upper mantle Pn velocity beneath most of the Baikalian belt is between 7.9 and 8.1 km/s with a local high of 8.6 km/s in the central part of the belt constrained by one seismic profile only (Fig. 13).

The Paleozoic collisional crust includes two provinces in the central-western and southern parts of the WSB, which were formed during successive subduction and collision events, involving accretion of island-arcs and micro-continents, regional magmatism and metamorphism. Regions affected by the Caledonian orogeny (the southern parts of the WSB) have a relatively thin crust (ca. 35–40 km) with a highly heterogeneous crustal structure which, in general, is similar to those parts of the Baikalides which did not experience strong extension. Similar to the southern Baikalides, the upper crust is thinned to less than 5 km, whereas the lower crust often exceeds 20–25 km in thickness (Fig. 10). Consequentially, the average Vp-velocities in the crystalline basement are also high, ca. 6.8 km/s (Fig. 8b). The Pn velocity shows a mosaic pattern related to the complex geodynamic evolution of the region.

Most of the Hercynides of the WSB have been significantly modified by Triassic rifting and have a ca. 30–35 km thick crystalline crust below a 2–5 km thick sedimentary cover with local deep grabens. The crustal structure of the rifted blocks is discussed in detail in the next section. Structure of the (non-rifted) Hercynian crust along the Urals is very similar to the crust of the (Proterozoic) Uvat–Khantymansiysk median massif: the crust is 35–40 km thick and thickens to 45 km towards the Urals orogen, the sedimentary cover is 1–3 km thick, the upper and middle crust is thick (10–15 km), the lower crust is thin (>10 km), and no high-velocity (Vp ~ 7.2–7.6 km/s) lowermost crustal layer is observed. As a consequence, the average basement Vp velocity is low (6.4–6.6 km/s). The Pn velocity is very heterogeneous and ranges from 7.9 km/s to, locally, 8.5 km/s.

5.5. Rifted crust of the WSB

Triassic rifting has significantly affected the crustal structure of the WSB, but to a different extent in different parts of the basin. The crust of the WSB is highly variable but, on the whole, significantly thicker (40 km) than expected from comparison with other large Phanerozoic sedimentary basins around the world (Roberts and Bally, 2012). Moho deepening (to 43–48 km) is observed mainly along the southern and central Urals and locally at the southern terminus of the Ob rift (Fig. 7a). Two prominent Moho uplifts (33 km depth) are observed in the southern part of the basin and in the northern part of the Ob rift system. The belt of ca. 42 km thick crust between thin crust in the north and in the south of the WSB approximately corresponds to a small (but the only) topographic anomaly of the WSB, the Sibirskie Uvaly high at ca. 62–63 N (Fig. 1). This high correlates with the belt of a relatively thick crystalline crust (35–37 km, Fig. 7b). In general, the thickness of the crystalline crust ranges from ca. 40 km in the southern blocks of the Baikalian and Caledonian orogeny (with local highs of 44 km) to ca. 25 km in local lows in the north (Fig. 7b).

The Permian-Triassic Ob rift system in the center of the WSB is formed by several rifts, including the Koltogory–Urengoi, Khudosei, Khudottei, Agan, Ust'Tym, Chuzik, and the Irtysh rifts and grabens (Pavlov, 1995). Except for the Irtysh rift, all major rifts of the West Siberian basin have a N–S or NE–SW orientation and each of them forms a separate graben—up to a few tens of kilometers wide and up to a few hundreds of kilometers long, symmetrical in cross-section, and bounded by steep faults (e.g. Aplonov, 1995). Importantly, most of the rifts have been mapped mainly by potential field (gravity and magnetic) methods (Allen et al., 2006). As a result, there are significant differences in the reported geometries and ages of the West Siberian graben system. Regional seismic profiles (mostly shallow exploration) show little evidence for any substantial rift system, except for the Pur–Taz area and the Kara sea where large grabens are observed in shallow seismic models (Peterson and Clarke, 1991; Shipilov and Tarasov, 1998; Vyssotski et al., 2006).

The present analysis indicates a complicated crustal structure of the Triassic rift system of the WSB. The top of the WSB basement is tilted towards the Arctic ocean; the thickness of the sedimentary cover increases from ca. 2–4 km in the south to more than 10 km at the Arctic coast and to 10–20 km in the Kara Sea basin. A deep basement depression (>12 km) is associated with the Khudosei rift. There is a significant difference in the crustal structure between the northern and southern parts of the rift system with crustal thicknesses of 35–40 km and 40–43 km, respectively. While the north-axial part of the Ob rift system can be clearly traced in the crustal structure by the presence of the high-velocity LMC and low Pn velocity, the southern part of the Ob rift system and the smaller rift branches cannot be distinguished in the seismic models. The most extended crust is observed in the Pur–Gydan depression in the north of the WSB where the upper crust is absent and the high-

velocity LMC is anomalously thick (12–17 km) in the central part of the depression. The presence of seismically fast and dense underplating material may provide an efficient mechanism for basin subsidence (Artyushkov and Baer, 1986), similar to other basins (Sandrin and Thybo, 2008). Extremely high average basement Vp velocity at the northern border between the SC and the WSB around 80E/70N, at the triple junction of the rift system of the WSB and its extension into the Yenisey–Khatanga trough, indicate the presence of magmatic intrusions in the crust and basaltic underplating. We speculate that this anomaly can indicate the source zone of the Siberian LIP.

The presence of three relict paleo-oceanic basins within the WSB preserved since the closure of the Paleozoic Khanty–Mansi ocean, the Nadym (64–66N/78–80E), Surgut (60–62N/77–80E), and Nyurol (56–59N, 86–89E) has been proposed by a number of authors. Basalts with composition similar to back-arc basins, sampled in few deep boreholes in these basins, were interpreted as ophiolites (Ignatova, 1966). The borehole data, together with a vertical change in sediment composition, a thin crust with 8–12 km of sediments, and positive gravity anomalies were used to argue for an oceanic origin of these basins (Aplonov, 1995; Demenitskaya, 1975; Ignatova, 1966; Peyve, 1969).

The present compilation allows for addressing the nature of the crust (continental versus oceanic) in these areas. The Nadym basin is crossed by profile BB′ (at the western end of the profile, Fig. 12), whereas the Surgut and Nyurol basins are crossed by profile FF′ (the south-central parts). The crustal structure of the Nadym basin is clearly anomalous as compared to a normal three-layer continental crust, given that the upper granitic crust is thinned to the near-zero values. The origin of the crust in the other two proposed relict basins is more speculative; the upper crust beneath both of them is thinned but still clearly present (Fig. 10a). The zone of increased average basement P-velocities (Fig. 8b) does not fully correlate with the chain of the proposed relic paleo-oceanic basins. Although seismic models apparently favor interpretation of the crustal structure of, at least the Nadym basin, as oceanic, we consider it a premature conclusion since more data (including deep drill data reaching the basement) are needed to prove the hypothesis.

The upper mantle Pn velocity in most of the WSB is surprisingly high, around 8.2 km/s, with local highs (8.3–8.4 km/s) along the southern and northern parts of the Urals. An isolated high-Pn velocity anomaly (8.4 km/s) in the center of the WSB seems to be unrelated to the major rift systems but rather with the Surgut basin. A belt of low-Pn velocity ($\leq$8.05 km/s) is observed in the northern and eastern parts of the WSB (Fig. 13); it spatially correlates with a belt of high ($>$6.7 km/s) average basement Vp velocities (Fig. 8b). Low Pn velocities under the axial part of the Ob rift system may be indicative of presently high upper mantle temperature.

5.6. Crustal reflectivity

Increased lower crustal reflectivity has been observed at ten seismic profiles included into the SibCrust model (note that some profiles do not provide information on crustal reflectivity). Regions with observed lower crustal reflectivity include the Yenisey–Khatanga trough, the Lena–Anabar trough, the Tunguska basin, the Mirnensk–Aihal High (Fig. 1), the southern flank of the Viluy basin, the northern part of the WSB, and the Norilsk region in the north-western corner of the SC. All regions with observed lower crustal reflectivity have undergone major extension or have been significantly affected by trap magmatism, suggesting compositional layering as origin of crustal reflectivity. In contrast, the lower crust of the Precambrian shields (Aldan and Anabar), when crossed by the same profiles, is nonreflective. Moho reflectivity is confidently present at all of the seismic profiles.

5.7. Statistical correlation of crustal parameters

We provide a statistical analysis of the crustal structure in order to examine potential correlations between the various parameters and with crustal ages as well as to distinguish possible trends in crustal evolution. As expected, the average crustal velocity increases with the thickness of the lower and lowermost crustal layers and decreases significantly with an increase in thickness of sediments and the upper crustal layer (Fig. 15a). The thickness of sediments is anticorrelated with the thickness of the crystalline crust and is on average ca. 6 km in regions with thin (ca. 35 km) crust and ca. 2–3 km in regions with ca. 50 km thick crust (Fig. 15b, top line).

We find indication that all regions with a thick ($>$45 km) crust have a thick ($>$10 km) lower and lowermost crust (Fig. 15b). Such crust is more common in the SC rather than in the WSB (Fig. 9). An increase in the thickness of the lower(most) crust (crustal layers with Vp $>$ 6.8 km/s) usually correlates with an increase in the thickness of the high-velocity (Vp $>$ 7.2 km/s) LMC (Fig. 15c). The total thickness of the upper and middle crust appears to be anticorrelated with the total thickness of the lower(most) crust. As a result, crustal blocks with very thick lower crust should not necessarily have a deep Moho. Thick LMC, such as observed in the Yenisey–Khatanga and the Ob rifts, is likely to be produced by magmatic underplating, as demonstrated at several active and extinct rift zones (Lyngsie et al., 2007; Thybo and Nielsen, 2009; Thybo et al., 2000; White et al., 2008). Intrusion of basaltic magma into the entire crustal column may also be responsible for the apparent UC thinning observed in these and other extensional structures (the Viluy rift) as well as in the Paleozoic orogens: additions of high-velocity material (e.g. sills and dikes, not necessarily distinguishable seismically but often magnetically (Lyngsie and Thybo, 2007)) will increase seismic velocities and, as a consequence, the upper crustal layers may acquire seismic velocities typical of the middle crust. This mechanism provides an alternative explanation for the (true or apparent) absence of the upper crust in the Nadym, Surgut, and Nyurol basins, interpreted by some authors as relict oceanic blocks.

Moho depth is generally smaller in the WSB than the SC (Fig. 9a), as expected for extended basins, and there is a significant difference in thickness of crystalline crust between the two regions, with peak at ca. 32–34 km in the WSB and at ca. 38–40 km in the SC (Fig. 9b). The average seismic velocity in the entire crust approximately follows the same distribution for the Siberian craton and the West Siberian basin and has a strong bimodal pattern in the WSB with peaks at ca. 5.4 km/s in deep sedimentary basins and at ca. 6.2 km/s in southern parts of the basin (Fig. 9c). The same peaks are also observed in the SC, where additionally the peak at ca. 6.45 km/s is typical for the shield regions. Considering the thick sedimentary cover with low velocity in the basin, it may be surprising that average crustal velocities are somewhat similar in the WSB and the SC. However, there is a tendency that the average velocity of the crystalline crust is higher in the basin than in the cratonic parts (Fig. 9d) and compensates for the low velocities of the sedimentary sequences. This difference in average basement velocity is probably caused by a relatively higher degree of intrusion of mafic melts into the rifted crust and underplating in strongly extended areas of the WSB, although similar patterns may be expected for the extended crust within the craton.

The middle crust of the WSB and SC is essentially equally thick, whereas in the WSB the upper crust is thinner but the lower crust is thicker than in the SC (Fig. 11). Thickening of the lower crust in the WSB may indicate magmatic intrusions into the crust and crustal underplating, which causes increased average basement velocity (Fig. 9d).

We do not observe any direct correlation between the upper mantle Pn velocity and the overall crustal structure. However, the SibCrust model suggests some negative correlation between Pn velocity and the average velocity of consolidated crust (Fig. 15d). This would

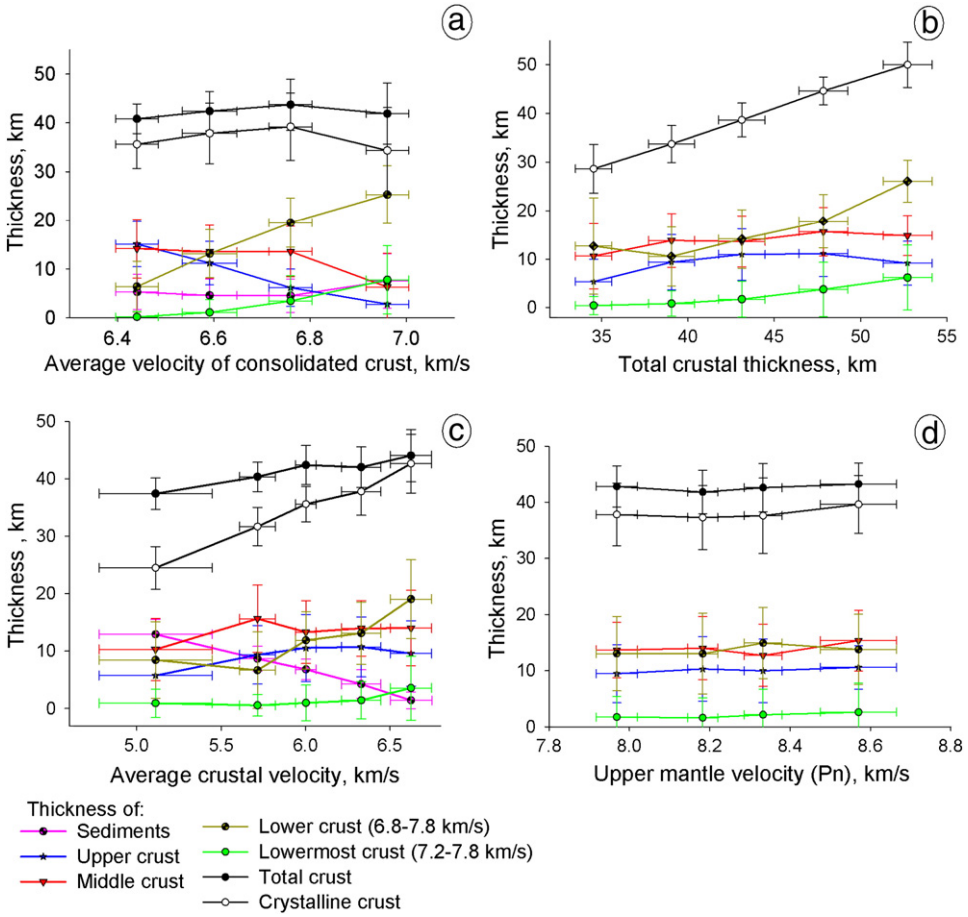

Fig. 15. Relationships between various crustal parameters based on the SibCrust seismic model: thicknesses of the crustal layers plotted against the average Vp velocity of the consolidated crust (a), against the Moho depth (b), against the average velocity of the crust including the sedimentary sequences (c), and against the upper mantle Pn velocity (d). Vertical and horizontal bars show standard deviation of the parameters based on the point data along the seismic profiles.

favor olivine anisotropy as the origin of the very high Pn velocity, whereas tectono-magmatic activity with high upper mantle temperatures (and, in some cases, with partial melting) is probably responsible for low Pn velocity and magmatic underplating, which eventually leads to the formation of a LMC.

We do not observe significant correlation between the crustal structure and the geological age of the crust (Fig. 16). There may be a tendency towards a thicker Archean than younger crust, and a possible decrease of depth to Moho with the age of the crust (Fig. 16a). However, this pattern is not systematically observed, and there are numerous small scale exceptions. Furthermore, all data points for the Paleoarchean are from the Aldan Foldbelt, which is subject to significant compression during the Phanerozoic. For this reason, the crustal structure of the oldest crustal terrane in Siberia may be non-representative of the Early Archean crust. The only robust trends are a general decrease of the basement thickness from the Precambrian to the Phanerozoic crust (Fig. 16b), and a pronounced thickening of the lower crust in the Paleoproterozoic-Neoarchean orogens (Yenisey Ridge) and the Baikalides (Fig. 16e).

6. Conclusions

We present a new compilation, SibCrust, of the seismic structure of the crust of Siberia (the Siberian craton and the West Siberian Basin) based on all available regional and local controlled-source seismic models and some receiver functions. The quality and reliability of the compiled seismic models are assessed in the database. Since the database is based solely on seismic results, it is suitable for application to the entire multitude of geophysical methods.

1. Our analysis reveals highly heterogeneous regional crustal structure at all scales. A very straightforward correlation is observed between tectonic setting and crustal (Vp) velocity structure.
   (a) Stable platform regions (most of the SC) have a ca. 45 km thick basement with a 0–3 km thick sedimentary cover. The crystalline basement is formed by three characteristic crustal layers with approximately the same (ca. 15 km) thickness. The absence of a high-velocity (Vp ~ 7.2–7.6 km/s) lowermost crustal layer is characteristic of stable platform regions in Siberia. We do not find unequivocal seismic evidence for the presence of proposed relic paleo-oceanic crustal blocks within the WSB.
   (b) Regions of extended crust in the SC and the WSB (mostly with Paleozoic-Mesozoic tectono-thermal ages) have an 18–40 km thick basement with an up to 10–20 km thick sedimentary cover. Decrease in the basement thickness is largely achieved through thinning (sometimes to near-zero) of the upper crustal layer. A high-velocity (Vp ~ 7.2–7.6 km/s) lowermost crustal layer (LMC), indicative of crustal underplating, is observed in the Yenisey–Khatanga and the Ob rifts (basins), but is absent in the Viluy basin of the SC.
   (c) Regions affected by the Baikalian and the Caledonian orogenies (the eastern and southern parts of the WSB) have a <5 km thick UC and 15–25 km thick LC, and consequentially, high average Vp-velocities in the crystalline crust (ca. 6.8 km/s). A lowermost crustal layer (LMC) with very high velocity is common.

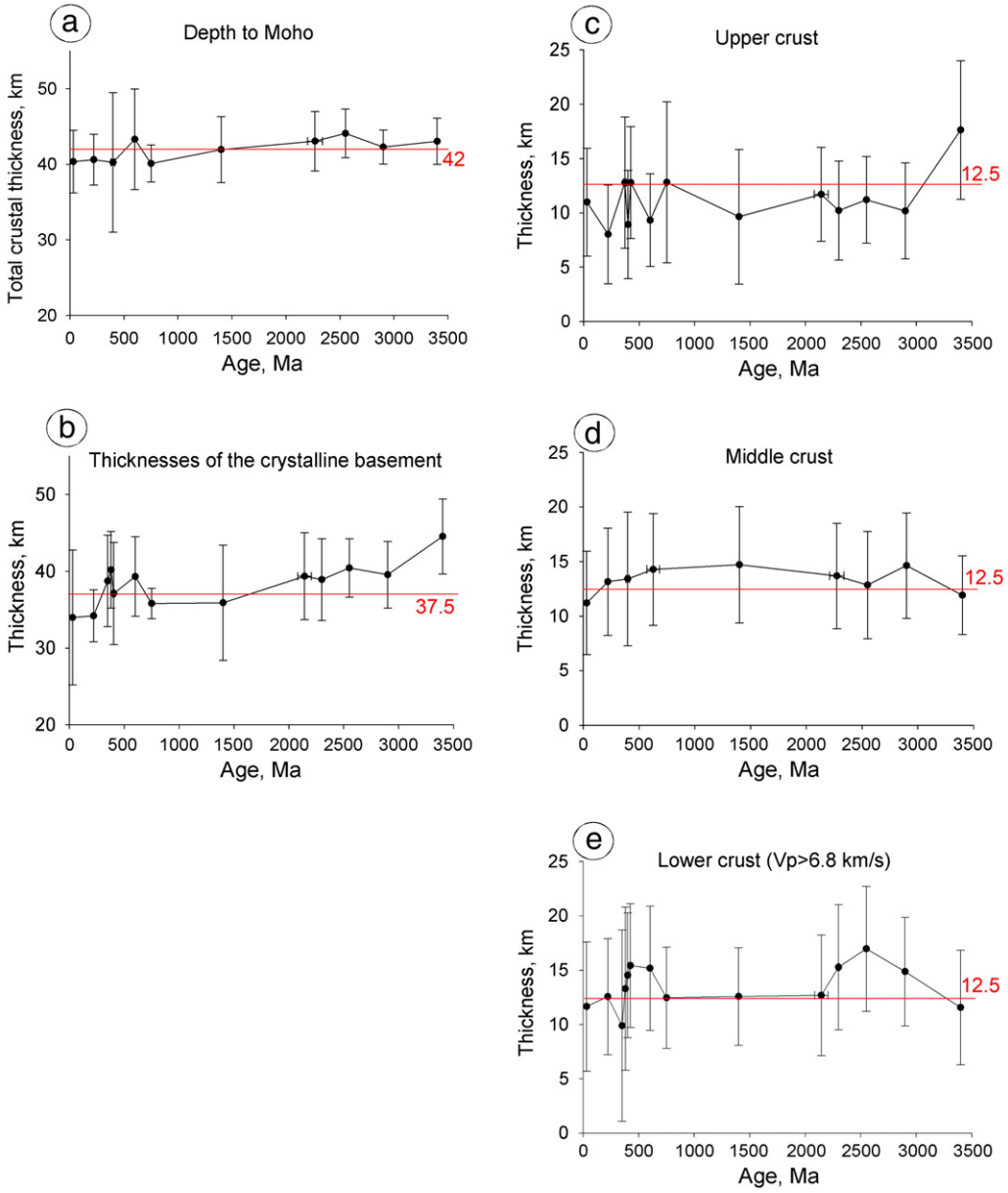

Fig. 16. Age dependence of various crustal parameters in Siberia based on the SibCrust seismic model: depth to Moho (a), thicknesses of the crystalline basement (b), upper crust (c), middle crust (d), and lower crust (Vp > 6.8 km/s) (e). The tectono-thermal age of the crust is based on data from Artemieva (2006). Vertical bars show standard deviation. The average values are calculated on a 1° × 1° grid, which corresponds to the resolution of the TC1 model. Note that all data points for the age 3.4 Ga are from the Aldan Foldbelt, while all data points for the age 2.55 Ga are from the Angara Foldbelt.

(d) Regions affected by the Hercynian orogeny (the WSB), but outside of the major rift system, have a ca. 30–35 km thick crystalline crust. The upper and lower crust are normal (10–15 km), and no high-velocity (Vp ~ 7.2–7.6 km/s) lowermost crustal layer is observed. Average Vp-velocities in the crystalline crust are normal (ca. 6.4–6.6 km/s). Similar crustal structure is typical for the suspected Proterozoic Uvat–Khantymansiysk median massif.

2. The Pn-velocity structure of the uppermost mantle is as variable as the velocity structure of the crust. (i) Reduced (7.8–8.0 km/s) Pn-velocities are typical for the Baikalian and Caledonian blocks, and are also observed in regions of Paleozoic-Mesozoic crustal extension (Ob and Yenisey–Khatanga rifts) and around major Siberian kimberlite provinces next to areas with extremely high Pn velocity. (ii) "Normal" (8.0–8.2 km/s) Pn-velocities are typical of most of the SC and the WSB. (iii) High (8.3–8.4 km/s, locally up to 8.5 km/s) Pn-velocities are reported for the Vilyu and Tunguska basins, the Angara–Lena structural terrace (north of the Baikal Rift), and the area around the Pai–Khoi ridge at the NW of the WSB. (iv) Abnormally high (8.6–8.9 km/s) Pn-velocities, of a possible compositional–anisotropic origin, are reported for the diamondiferous kimberlite province of the SC.
3. The average Moho depth is similar in the SC and the WSB (43.5 ± 3.7 km and 40.6 ± 3.7 km, respectively). The average thickness of the crystalline crust is, however, notably thicker in the SC than in the WSB, with the peaks at ca. 40 km and 32–34 km, respectively. The average velocity for the whole crust of Siberia is ca. 5.95–6.0 km/s, but with the high proportion of regions with velocities >6 km/s. The average crustal velocity has a bimodal distribution in the WSB and has an additional high-velocity (ca. 6.4 km/s) peak in the shields of the SC. For the crystalline crust, the average velocity is 6.65 km/s with extreme high velocities (6.9 km/s) below the most rifted northern part of the WSB, which may be caused by the presence of

magmatic intrusions and underplated material, possible associated with the source zone of the Siberian LIP.

Our new compilation of the crustal structure of the West Siberian Basin and the Siberian craton, SibCrust, can be downloaded from [www.lithosphere.info].

Acknowledgments

Several scientific libraries of the Russian Academy of Sciences, as well as the USGS (Menlo Park, CA) library have provided invaluable support in collecting original seismic publications. The authors acknowledge W.D. Mooney (USGS, Menlo Park) for provoking this study; E.D. Milstein and Y.M. Erinchek (both VSEGEI, Russia) are gratefully acknowledged for informative discussions on the regional seismic data coverage in Siberia. Constructive editorial and review comments helped to sharpen the presentation. YC and ZC funding through the grants of FNU-10-083081 (Denmark) and the Faculty of Science, University of Copenhagen to IMA is gratefully acknowledged. Handling Editor was Fabrizio Storti.

References

Al'mukhamedov, A.I., Medvedev, A.Ya., Kirda, N.P., Baturina, T.P., 1998. The Triassic volcanogenic complex of the Western Siberia. Doklady Earth Sciences 362 (7), 931–935.
Allen, M.B., Anderson, L., Searle, R.C., Buslov, M., 2006. Oblique rift geometry of the West Siberian basin: tectonic setting for the Siberian flood basalts. Journal of the Geological Society of London 163, 901–904.
Amante, C., Eakins, B.W., 2009. ETOPO1 1 Arc-Minute Global Relief Model: Procedures. Data Sources and Analysis. NOAA Technical Memorandum NESDIS NGDC-24 (19 pp., March).
Aplonov, S.V., 1988. An aborted Triassic ocean in West Siberia. Tectonics 7, 1103–1122.
Aplonov, S.V., 1995. The tectonic evolution of West Siberia: an attempt at a geophysical analysis. Tectonophysics 245, 61–84.
Arkhipov, S.A., 1971. Quaternary Period in the West Siberia. Nauka, Novosibirsk (in Russian).
Artemieva, I.M., 2006. Global 1 deg × 1 deg thermal model TC1 for the continental lithosphere: implications for lithosphere secular evolution. Tectonophysics 416, 245–277.
Artemieva, I.M., Meissner, R., 2012. Crustal thickness controlled by plate tectonics: a review of crust–mantle interaction processes illustrated by European examples. Tectonophysics 530–531, 18–49.
Artemieva, I.M., Mooney, W.D., 2001. Thermal structure and evolution of Precambrian lithosphere: a global study. Journal of Geophysical Research 106, 16387–16414.
Artemieva, I.M., Thybo, H., 2013. EUNAseis: A seismic model for Moho and crustal structure in Europe, Greenland, and the North Atlantic region. Tectonophysics 609, 97–153 (this volume).
Artemieva, I.M., Thybo, H., Kaban, M.K., 2006. Deep Europe today: geophysical synthesis of the upper mantle structure and lithospheric processes. In: Gee, D., Stephenson, R. (Eds.), European Lithosphere DynamicsGeological Society London Memoirs 32, 11–41.
Artyushkov, E.V., 1993. Physical Geotectonics. Nauka, Moscow (in Russian).
Artyushkov, E.V., Baer, M.A., 1986. Mechanism of formation of hydrocarbon basins—the West Siberia, Volga–Urals, Timan–Pechora basins and the Permian basin of Texas. Tectonophysics 122 (3–4), 247–281.
Avetisov, G.P., Golubkov, V.S., 1984. Deep structure of the central part of the Norilsk ore region from the MOVZ-DSS data. Sovetskaya Geologiya 10, 86–94.
Avetisov, G.P., Golubkov, V.S., 1996. Deep structure of the Norilsk area by the results of DSS. Geological and geophysical characteristics of the lithosphere of the Arctic region, St.- Petersburg, pp. 183–197.
Baldin, V.A., 2001. Geological structure and petroleum prospects of Upper Jurassic–Neocomian sediments in the western portion of the Yenisei–Khatanga trough. Cand. Sci. (Geol._Mineral.).VNIGNI, Moscow (Dissertation).
Bascou, J., Doucet, L.S., Saumet, S., Ionov, D.A., Ashepkov, I.V., Golovin, A.V., 2011. Seismic velocities, anisotropy and deformation in Siberian cratonic mantle: EBSD data on xenoliths from the Udachnaya kimberlite. Earth and Planetary Science Letters 304 (1–2), 71–84.
Bassin, C., Laske, G., Masters, G., 2000. The current limits of resolution for surface wave tomography in North America. Eos, Transactions of the American Geophysical Union 81, F897.
Bazanov, E.A., Pritula, Yu.A., Zabalueva, V.V., 1976. Development of main structures of the Siberian platform: history and dynamics. Tectonophysics 36 (1–3), 289–300.
Bekzhanov, G.R., Lyubetskiy, V.N., Polevaya, L.D., 1974. Characteristics of tectonic development of Kazakhstan (from geophysical data). International Geology Review 16 (8), 953–962.
Beloussov, V.V., Pavlenkova, N.I., Kvyatovskaya, G.N., 1991. Deep Structure of the USSR Territory. Nauka, Moscow.
Belyaevsky, N.A., 1973. The Structure of the Crust and Upper Mantle of the Seas and Oceans. NAUKA, Moscow.
Bochkarev, V.S., Brekhuntsov, A.M., Deshchenya, N.P., 2003. The Paleozoic and Triassic evolution of West Siberia (data of comprehensive studies). Russian Geology and Geophysics 44 (1–2), 120–143.
Bradley, D.C., 2008. Passive margins through earth history. Earth-Science Reviews 91, 1–26.
Braitenberg, C., Ebbing, J., 2009. New insights into the basement structure of the West Siberian Basin from forward and inverse modeling of GRACE satellite gravity data. Journal of Geophysical Research 114 (B06402), 15.
Brown, D., Juhlin, C., Alvarez-Marro, .N.J., Pe Rez-Estaun, A., Oslianski, A., 1998. The crustal-scale structure and geodynamic evolution of an arc–continent collision zone in the Southern Urals, Russia. Tectonics 2, 158–170.
Brown, D., Juhlin, C., Tryggvason, A., et al., 2002. The crustal architecture of the Southern and Middle Urals from the URSEIS, ESRU, and Alapaev reflection seismic profiles. In: Brown, D., Juhlin, C., Puchkov, V. (Eds.), Mountain Building in the Uralides: Pangea to Present: Geophysical Monographs, American Geophysical Union, 132, pp. 33–48.
Brown, D., Juhlin, C., Ayala, C., Tryggvason, A., Bea, F., Alvarez-Marron, J., Carbonell, R., Seward, D., Glasmacher, U., Puchkov, V., Perez-Estaun, A., 2008. Mountain building processes during continent–continent collision in the Uralides. Earth-Science Reviews 89 (3–4), 177–195.
Bulin, N.K., 1988. Deep structure of the east part of the Siberian platform from seismic data. Sovetskaya Geologiya 5, 58–66.
Bulin, N.K., 2003. Lateral velocity heterogeneity of the low part of the earth's crust for the Siberian territory. Regional Geology and Metallogeny 17, 66–73.
Bulin, N.K., Egorkin, A.V., 1994. Multiwaves deep seismic sounding in fine-scale in fine-scale investigation studies. Otechestvennaya Geologiya 4, 43–50.
Carbonell, R., et al., 1996. Crustal root beneath the Urals: wide-angle seismic evidence. Science 274 (5285), 222–224.
Carbonell, R., Gallart, J., Perez-Estaun, A., Diaz, J., Kashubin, S., Mechie, J., Wenzel, F., Knapp, J., 2000. Seismic wide-angle constraints on the crust of the southern Urals. Journal of Geophysical Research 105 (B6). http://dx.doi.org/10.1029/2000JB900048 (issn: 0148-0227).
Christensen, N.I., Mooney, W.D., 1995. Seismic velocity structure and composition of the continental crust: a global view. Journal of Geophysical Research 100 (B6), 9761–9788.
Closs, H., Behnke, C., 1963. Progress in the use of seismic methods in the exploration of the Earth's crust. International Geology Review 5 (8), 945–956.
Clowes, R.M., Burianyk, M.J.A., Gorman, A.R., et al., 2002. Crustal velocity structure from SAREX, the Southern Alberta Refraction Experiment. Canadian Journal of Earth Sciences 39, 351–373. http://dx.doi.org/10.1139/E01-070.
Courtillot, V., Kravchinsky, V.A., Quidelleur, X., Renne, P.R., Gladkochub, D.P., 2010. Preliminary dating of the Viluy traps (Eastern Siberia): eruption at the time of Late Devonian extinction events? Earth and Planetary Science Letters 300, 239–245.
Davis, G.L., Sobolev, N.V., Kharkiv, A.D., 1980. New data on ages of Yakutian kimberlites after uranium–lead zircon method. Doklady Akademii Nauk SSSR 254 (1), 175–179 (in Russian).
De Wit, M., Stankiewicz, J., 2013. 3.5 billion years of reshaped Moho, southern Africa. Tectonophysics 609, 675–689 (this volume).
De Wit, M.J., de Ronde, C.E.J., Tredoux, M., Roering, C., Hart, R.J., Armstrong, R.A., Green, R.W.E., Peberdy, E., Hart, R.A., 1992. Formation of an Archaean continent. Nature 357, 553–562.
Demenitskaya, R.M., 1975. The Earth's Crust and Mantle. Nedra, Moscow (in Russian).
Downes, H., 1993. The nature of the lower continental crust of Europe: petrological and geochemical evidence from xenoliths. Physics of the Earth and Planetary Interiors 79, 195–218.
Drachev, S.S., Savostin, L.A., Groshev, V.G., Bruni, I.E., 1998. Structure and geology of the continental shelf of the Laptev Sea, Eastern Russian Arctic. Tectonophysics 298, 357–393.
Drachev, S.S., Malyshev, N.A., Nikishin, A.M., 2010. Tectonic history and petroleum geology of the Russian Arctic Shelves: an overview. Geological Society, London, Petroleum Geology Conference series, 7, pp. 591–619.
Druzhinin, V.S., Egorkin, A.V., Kashubin, S.N., 1990. New data on the deep structure of the Urals and adjacent regions from DSS studies. Doklady Akademii Nauk SSSR 315 (5), 1086–1090 (in Russian).
Druzhinin, V.S., Kashubin, S.N., Kashubina, T.V., Kolmogorova, V.A., Parygin, G.V., Rybalka, A.V., Tiunova, A.M., 1997. The main features of the interface between the crust and the upper mantle in the Middle Urals (in the vicinity of the deep drillhole SG-4). Tectonophysics 269, 259–267.
Duchkov, A.D., Lysak, S.V., Balobaev, V.T., 1987. Thermal Field of Siberia Interiors. Nauka, Novosibirsk (In Russian).
Durrheim, R.J., Mooney, W.D., 1991. Archean and proterozoic crustal evolution—evidence from crustal seismology. Geology 19 (6), 606–609.
Echtler, H.P., Stiller, M., Steinhoff, F., et al., 1996. Preserved collisional crustal structure of the Southern Urals revealed by vibroseis profiling. Science 274, 224–226.
Egorkin, A.V., 1991. Crustal structure according to seismic transects. Deep Structure of the Territory of the USSR. Moscow, pp. 118–134 (in Russian).
Egorkin, A.V., 1999. Study on the mantle at the super long geotraverses. Physics of the Earth and Planetary Interiors 7 (8), 114–130.
Egorkin, A.V., Zuganov, S.K., Pavlenkova, N.A., Chernyshev, N.M., 1987. Results of lithospheric studies from long-range profiles in Siberia. Tectonophysics 140 (1), 29–47.
Egorkin (Yegorkin), Pavlenkova, N.I., Kvyatkovskaya, G.N., 1992. Crustal structure along seismic geotraverses. International Geology Review 34 (4), 345–444.
Egorov, A.S., Gur'ev, G.A., Zotova, I.F., Kirikov, D.A., Movchan, I.B., Chistyakov, D.N., 2000. Geology–geophysics and geodynamic model of the lithosphere along the line of geotraverse Rubcovsk–Nevelskii. Regional Geology and Metallogeny 10, 143–151.
Erinchek, Yu.M., 2009. Crustal Structure of the Territory of Russia. VSEGEI Compilation, St. Petersburg (Personal communication).

Fedorenko, V.A., Lightfoot, P.C., Naldrett, A.J., Czamanske, G.K., Hawkesworth, C.J., Wooden, J.L., Ebel, D.S., 1996. Petrogenesis of the Siberian flood-basalt sequence at Noril'sk, north central Siberia. International Geology Review 38, 99–135.
Fokin, P.A., Nikishin, A.M., Ziegler, P.A., 2001. Peri-Uralian and Peri-Palaeo-Tethyan rift systems of the East European Craton. Memoires du Museum National d'Histoire Naturelle 186, 347–368.
Friberg, M., Juhlin, C., Roth, J., Horstmeyer, H., Rybalka, A., Bliznetsov, M., 2001. Europrobe seismic reflection profiling across the eastern Middle Urals and West Siberian Basin. Terra Nova 14, 7–13.
Gao, S., Davis, P.M., Liu, H., Slack, P.D., Zorin, Y.A., Logatchev, N.A., Kogan, M., Burkholder, P.D., Meyer, R.P., 1994. Asymmetric upward of the asthenosphere beneath the Baikal rift zone, Siberia. Journal of Geophysical Research 99, 15319–15330.
Gladkochub, D., Pisarevsky, S.A., Donskaya, T., Natapov, L.M., Mazukabzov, A., Stanevich, A., Slkyarov, E., 2006. Siberian craton and its evolution in terms of Rodinia hypothesis. Episodes 29 (3), 169–174.
Grachev, A., Kaban, M.K., 2006. Factors responsible for the high position of the Siberian platform. Izvestiya—Physics of the Solid Earth 42 (12), 987–998.
Gradstein, F.M., Ogg, J.G., Schmitz, M.D., Ogg, G.M., 2012. The Geologic Time Scale 2012. Elsevier (1176 pp.).
Griffin, W.L., Ryan, C.G., Kaminsky, F.V., O'Reilly, S.Y., Natapov, L.M., Win, T.T., Kinny, P.D., Ilupin, I.P., 1999. The Siberian lithosphere traverse: mantle terranes and the assembly of the Siberian craton. Tectonophysics 310, 1–35.
Gupta, S., Rai, S.S., Prakasam, K.S., Srinagesh, D., Bansal, B.K., Chadha, R.K., Priestley, K., Gaur, V.K., 2003. The nature of the crust in southern India: implications for Precambrian crustal evolution. Geophysical Research Letters 30 (8), 1419.
Ignatova, V.F., 1966. On a possible oceanic crust in the central parts of the intracontinental depressions, such as West Siberia. In: Kosygin, Yu.A. (Ed.), Geological Problems of the Pacific Belt. Vladivostok, pp. 45–50 (in Russian).
Ilupin, I.P., Vaganov, V.I., Prokpuck, B.I., 1990. Kimberlites. Nedra, Moscow (in Russian).
Ivanova, N.M., Sakoulina, T.S., Roslov, Y.V., 2006. Deep seismic investigation across the Barents–Kara region and Novozemelskiy Fold Belt (Arctic Shelf). Tectonophysics 420, 123–140.
Ivanova, N.M., Sakulina, T.S., Belyaev, I.V., et al., 2011. Depth model of the Barents and Kara seas according to geophysical surveys results. In: Spencer, A.M., Embry, A.F., Gautier, D.L., Stoupakova, A.V., Sørensen, K. (Eds.), Arctic Petroleum GeologyGeological Society London Memoirs 35, 209–221. http://dx.doi.org/10.1144/M35.12 (Chapter 12).
Jahn, B.-M., Gruan, G., Capdevila, R., Cornichet, J., Nemchin, A., Pidgeon, R., Rudnik, V.A., 1998. Archean crustal evolution of the Aldan Shield, Siberia: geochemical and isotopic constraints. Precambrian Research 91 (3–4), 333–363.
Jarchow, C.M., Thompson, G.A., 1989. The nature of the Mohorovicic-discontinuity. Annual Review of Earth and Planetary Sciences 17, 475–506.
Juhlin, C., Knapp, J.H., Kashubin, S., Bliznetsov, M., 1996. Crustal evolution of the Middle Urals based on seismic reflection and refraction data. Tectonophysics 264 (1–4), 21–34.
Juhlin, C., Friberg, M., Echtler, H., et al., 1998. Crustal structure of the Middle Urals: results from the (ESRU) Europrobe seismic reflection profiling in the Urals experiments. Tectonics 17 (5), 710–725.
Kashubin, S., Juhlin, C., Friberg, M., et al., 2006. Crustal structure of the Middle Urals based on seismic reflection data. In: Gee, D.G., Stephenson, R.A. (Eds.), European Lithosphere DynamicsGeological Society London Memoirs 32, 427–442.
Kennett, B.L.N., Salmon, M., Saygin, E., 2011. AusMoho: the variation of Moho depth in Australia. Geophysical Journal International 187 (2), 946–958.
Khain, V.E., 2001. Tectonics of Continents and Oceans (year 2000). Nauchnyi Mir, Moscow.
Klets, A.G., Budnikov, I.V., Kutygin, R.V., Biakov, A.S., Grinenko, V.S., 2006. The Permian of the Verkhoyansk–Okhotsk region, NE Russia. Journal of Asian Earth Sciences 26 (3–4), 258–268.
Knapp, J.H., et al., 1998. Seismic reflection fabrics of continental collision and post-orogenic extension in the Middle Urals, central Russia. Tectonophysics 288 (1–4), 115–126.
Kobussen, A.F., Christensen, N.I., Thybo, H., 2006. Constraints on seismic velocity anomalies beneath the Siberian craton from xenoliths and petrophysics. Tectonophysics 425 (1–4), 123–135.
Kontorovich, A.E., Nesterov, I.I., Salmanov, F.K., Surkov, V.S., Trofimuk, A.A., Ervie, Yu.G., 1975. Geology of Oil and Gas of the West Siberia. Nedra, Moscow.
Korja, A., Korja, T., Luosto, U., Heikkinen, P., 1993. Seismic and geoelectric evidence for collisional and extensional events in the Fennoscandian shield—implications for Precambrian crustal evolution. Tectonophysics 219, 129–152.
Korsman, K., Korja, T., Pajunen, M., et al., 1999. The GGT/SVEKA transect: structure and evolution of the continental crust in the Paleoproterozoic Svecofennian orogen in Finland. International Geology Review 41, 287–333.
Kostuychenko, S.L., Egorkin, A.V., 1994. Intracrustal structure of the northern East Europe platform. Exploration and Protection of Mineral Resources 10, 12–15.
Kostuychenko, S.L., Egorkin, A.V., Solodilov, L.N., 1998. The features of the structure of the Urals's lithosphere by the results of multiwave deep seismic sounding. Geotectonics 4, 3–18.
Kostyuchenko, S.L., 2000. Structure of the crust and deep mechanisms of formation of Arctic sedimentary basins of Siberia. Regional Geology and Metallogeny 10, 125–135.
Kovylin, V.M., 1985. Block structure of the West Siberian basin and oil-gas-bearing. Soviet Geology 2, 77–86.
Krylov, S.V., Mishenkin, B.P., Rudnitskii, L.A., Suvorov, V.D., 1974a. Characteristic of the West-Siberian region and the deep seismic sounding data. The Structure of the Earth's Crust in Western Siberia (Results of Deep Seismic Sounding), Novosibirsk, pp. 6–15.
Krylov, S.V., Suvorov, V.D., Rudnickii, A.L., 1974b. Block structure of the earth's crust of the West Siberia. Structure of the West Siberia (By Results of the Deep Seismic Sounding), Novosibirsk.
Kukkonen, I.T., 1998. Temperature and heat flow density in a thick cratonic lithosphere: the Sveka transect, central Fennoscandian Shield. Journal of Geodynamics 26, 111–136.
Kunin, N.Ya., Ioganson, L.I., 1984. Geophysical Characteristics and Structure of the Crust of Western Siberia. Nauka, Moscow.
Kushnir, D.G., 2006. Paleozoic swells in the north of central and western Siberia. Geotectonics 40 (5), 399–404.
Kwadiba, M.T.O.G., Wright, C., Kgaswane, E.M., Simon, R.E., Nguuri, T.K., 2003. Pn arrivals and lateral variations of Moho geometry beneath the Kaapvaal craton. In: Jones, A.G., Carlson, R.W., Grutter, H. (Eds.), Lithos Special Issue: The Slave–Kaapvaal Workshop: A Tale of Two Cratons, 71, pp. 393–411.
Logatchev, N.A., Zorin, Y.A., 1987. Evidence and cause of the two-stage development of the Baikal rift. Tectonophysics 143, 225–234.
Lyngsie, S.B., Thybo, H., 2007. A new tectonic model for the Laurentia–Avalonia–Baltica sutures in the North Sea: a case study along MONA LISA profile 3. Tectonophysics 429, 201–227.
Lyngsie, S.B., Thybo, H., Lang, R., 2007. Rifting and lower crustal reflectivity: a case study of the intracratonic Dniepr–Donets rift zone, Ukraine. Journal of Geophysical Research 112, B12402.
Macelwane, J.B., 1951. Evidence on the interior of the earth derived from seismic studies, In: Gutenberg, B. (Ed.), Internal Constitution of the Earth, 2nd ed. Dover Publ., Inc., pp. 227–304 (Chapter X).
Mall, D.M., Chandrakala, K., Kumar, A.S., Sarkar, D., 2012. Sub-crustal LVZ below Dharwar craton, India: an evidence for mantle metasomatism and tectonothermal activity in the Archean crust. Precambrian Research 208, 161–173.
McKerrow, W.S., Mac Niocaill, C., Dewey, J.F., 2000. The Caledonian Orogeny redefined. Journal of the Geological Society 157, 1149–1154.
Mechie, J., Egorkin, A.V., Fuchs, K., Ryberg, T., Solodilov, L.N., Wenzel, F., 1993. P-wave mantle velocity structure beneath northern Eurasia from long-range recordings along the profile Quartz. Physics of the Earth and Planetary Interiors 79, 269–286.
Meissner, R., 1986. The Continental Crust. Academic Press, Orlando.
Metelkin, D.V., Gordienko, I.V., Klimuk, V.S., 2007. Paleomagnetism of Upper Jurassic basalts in Transbaikalia: new data on the time of closing the Mongol–Okhotsk Ocean and beginning of Mesozoic intraplate tectonics in central Asia. Russian Geology and Geophysics 48 (10), 1061–1073.
Milanovskiy, E.E., 1996. Geologiya Rossii i blizhnego zarubezh'ya (Severnaya Evraziya). Geology of Russia and Near Abroad, North Eurasia. Izd. Mosc. Univ., Moscow.
Mooney, W.D., Detweiler, S., 2005. Global Seismic Profiles Catalogue (GSC). USGS, Menlo Park, CA (Personal communication).
Mooney, W.D., Laske, G., Masters, T.G., 1998. CRUST 5.1: a global crustal model at 5 × 5. Journal of Geophysical Research 103 (B1), 727–747.
Morozov, I.B., Morozova, E.A., Smithson, S.B., Solodilov, L.N., 1998. 2-D image of seismic attenuation beneath the deep seismic sounding profile "Quartz". Pure and Applied Geophysics 153, 311–343.
Morozov, I.B., Smithson, S.B., Solodilov, L.N., 2002. Imaging crustal structure along refraction profiles using multicomponent recordings of first-arrival coda. Bulletin of Seismological Society of America 92 (8), 3080–3086.
Morozova, E.A., Morozov, I.B., Smithson, S.B., Solodilov, L., 2000. Lithospheric boundaries and upper mantle heterogeneity beneath Russian Eurasia: evidence from the DSS profile QUARTZ. Tectonophysics 329, 333–344.
Nair, S.K., Gao, S.S., Liu, K.H., Silver, P.G., 2006. Southern African crustal evolution and composition: constrains from receiver function studies. Journal of Geophysical Research 111, BO2304.
Nguuri, T.K., Gore, J., James, D.E., Webb, S.J., Wright, C., Zengeni, T.G., Gwavava, O., Snoke, J.A., 2001. Crustal structure beneath southern Africa and its implications for the formation and evolution of the Kaapvaal and Zimbabwe cratons. Geophysical Research Letters 28 (13), 2501–2504.
Nielsen, C., Thybo, H., 2009. Lower crustal intrusions beneath the southern Baikal Rift Zone: evidence from full-waveform modelling of wide-angle seismic data. Tectonophysics 470, 298–318.
Nielsen, C., Thybo, H., 2009. No Moho uplift below the Baikal Rift Zone: evidence from a seismic refraction profile across southern Lake Baikal. Journal of Geophysical Research 114. http://dx.doi.org/10.1029/2008JB005828.
Nielsen, L., Thybo, H., Solodilov, L.N., 1999. Seismic tomographic inversion of Russian PNE data along profile Craton. Geophysical Research Letters 26 (22), 3413–3416.
Nielsen, L., Thybo, H., Egorkin, A.V., 2002. Implications of seismic scattering below the 8 degrees discontinuity along PNE profile Kraton. Tectonophysics 358, 135–150.
Nikishin, A.M., Ziegler, P.A., Stephenson, R.A., Cloetingh, S.A.P.L., Furne, A.V., Fokin, P.A., Ershov, A.V., Bolotov, S.N., Korotaev, M.V., Alekseev, A.S., Gorbachev, V.I., Shipilov, E.V., Lankreijer, A., Bembinova, E.Yu., Shalimov, I.V., 1996. Late Precambrian to Triassic history of the East European Craton: dynamics of sedimentary basin evolution. Tectonophysics 268 (1–4), 23–63.
Nikishin, A.M., Sobornov, K.O., Prokopiev, A.V., Frolov, S.V., 2010. Tectonic evolution of the Siberian Platform during the Vendian and Phanerozoic. Moscow University Geology Bulletin 65 (1), 1–16.
Nui, F., James, D.E., 2002. Constraints on the formation and composition of crust beneath the Kaapvaal craton from Moho reverberations. Earth and Planetary Science Letters 200, 121–130.
Nutman, A.P., Chernyshev, I.V., Baadsgaard, H., Smelov, A.P., 1992. The Aldan Shield of Siberia, USSR: the age of its Archaean components and evidence for widespread reworking in the mid-Proterozoic. Precambrian Research 54 (2–4), 195–210.
O'Reilly, S.Y., Griffin, W.L., 1985. A xenolith derived geotherm for southeastern Australia and its geophysical implications. Tectonophysics 111, 41–63.
Parfenov, L.M., Kuzmin, M.I., 2001. Tektonika, geodinamika i metallogeniya territorii Respubliki Sakha (Yakutiya)/Tectonics, Geodynamics, and Metallogeny of the Sakha (Yakutia) Republic. MAIK Nauka/Interperiodika, Moscow.
Pavlenkova, N.I., 1996. Crust and upper mantle structure in northern Eurasia from seismic data. Advances in Geophysics 37, 1–121.

Pavlenkova, G.A., 1998. Seismic model of the lithosphere along the Rift profile. Razvedka i Ohrana Nedr 6–11.
Pavlenkova, G.A., 2000. New data about the structure of the earth's crust and upper mantle for the QUARTC profile. Exploration and Protection of Mineral Resources 2, 11–15.
Pavlenkova, G.A., Pavlenkova, N.I., 2006. Upper mantle structure of the Northern Eurasia from peaceful nuclear explosion data. Tectonophysics 416, 33–52.
Pavlenkova, N.I., Pavlenkova, G.A., Solodilov, L.N., 1996. High velocity in the uppermost mantle of the Siberian craton. Tectonophysics 262 (1), 51–65.
Pavlenkova, N.I., Priestley, K., Cipar, J., 2002. D model of the crust and uppermost mantle along rift profile, Siberian craton. Tectonophysics 355, 171–186.
Pavlov, Y.A., 1995. On recognition of rift structures in the basement of the West Siberian plate. Geotectonics 29 (3), 213–223.
Peterson, J.A., Clarke, J.W., 1991. Geology and Hydrocarbon Habitat of the West Siberian Basin. American Association of Petroleum Geologists.
Petrov, O.V., Kostyuchenko, S.L., 2002. Deep sedimentary troughs of Siberia as a result of influence minor mantle plumes on the earth's lithosphere. Regional Geology and Metallogeny 15, 58–74.
Peyve, A.V., 1969. Oceanic crust of the geological past. Geotectonics 6, 3–21 (in Russian).
Pisarevsky, S.A., Natapov, L.M., 2003. Siberia and Rodinia. Tectonophysics 375, 221–245.
Priestley, K., Debayle, E., 2003. Seismic evidence for a moderately thick lithosphere beneath the Siberian platform. Geophysical Research Letters 30 (3), 1118.
Prokopiev, A.V., Toro, J., Miller, E.L., et al., 2008. The Paleo Lena River—200 M.Y. of transcontinental zircon transport in Siberia. Geology 36 (9), 699–702.
Puchkov, V.N., 1997. Structure and geodynamics of the Uralide orogen. In: Burg, J.P., Ford, M. (Eds.), Orogeny Through TimeGeological Society, London, Special Publications 121, 201–236.
Puzyrev, N.N., Krylov, S.V., 1977. Main results of regional seismic studies in Siberia. Geophysical Methods in the Study of the Siberian Crust 249, 17–28.
Reichow, M.C., Saunders, A.D., White, R.V., Pringle, M.S., Al'Mukhamedov, A.I., Medvedev, A.I., Kirda, N.P., 2002. 40Ar/39Ar dates from the West Siberian basin: Siberian flood basalt province doubled. Science 296, 1846–1849.
Roberts, D.G., Bally, A.W. (Eds.), 2012. Regional Geology and Tectonics: Principles of Geologic Analysis. Elsevier (906 pp., ISBN 13: 978-0-444-53042-4.).
Romanyuk, T.V., 1995. The seismic-density modeling of the tectonosphere for the Craton profile. Exploration and Protection of Mineral Resources 5, 24–31.
Rosen, O.M., 2002. Siberian craton—a fragment of a Paleoproterozoic supercontinent. Russian Journal of Earth Sciences 4 (2), 103–119.
Rosen, O.M., 2003. The Siberian Craton: tectonic zonation and stages of evolution. Geotectonics 37 (3), 175–192.
Rosen, O.M., Condie, K.C., Natapov, L.M., Nozhkin, A.D., 1994. Paleoproterozoic evolution of the Siberian craton: a preliminary assessment. In: Condie, K.C. (Ed.), Archean Crustal Evolution. Elsevier, Amsterdam, pp. 411–459.
Rosen, O.M., Manakov, A.V., Serenko, V.P., 2005. Paleoproterozoic collisional system and diamondiferous lithospheric keel of the Yakutian Kimberlite Province. Russian Geology and Geophysics 46 (12), 1237–1251.
Roslov, Yu.V., Sakoulina, T.S., Pavlenkova, N.I., 2009. Deep seismic investigations in the Barents and Kara Seas. Tectonophysics 472, 301–308.
Roy, S., Mareschal, J.-C., 2011. Constraints on the deep thermal structure of the Dharwar craton, India, from heat flow, shear wave velocities, and mantle xenoliths. Journal of Geophysical Research 116, B02409.
Roy, S., Rao, R.U.M., 2003. Towards a crustal thermal model for the Archaean Dharwar craton, southern India. Physics and Chemistry of the Earth 28, 361–373.
Rudkevich, M.Ya., 1974. Paleotectonic Criteria for Hydrocarbon Occurrences. Nedra, Moscow (184 pp. (in Russian)).
Rudnick, R.L., Fountain, D.M., 1995. Nature and composition of the continental crust: a lower crustal perspective. Reviews of Geophysics 33, 267–309.
Ryaboy, V., 1989. Upper mantle structure studies by explosion seismology in the USSR. Monograph series on Soviet Union, 138. Delphic Associates.
Rybalka, V., Kashubin, S. (Eds.), 1992. GRANIT Transect. Methods and Results of Investigations. URGK I UTP VNTGeo, Ekaterinburg (113 pp. (in Russian)).
Ryberg, T., Wenzel, F., Mechie, J., Egorkin, A., Fuchs, K., Solodilov, L., 1996. Two-dimensional velocity structure beneath northern Eurasia derived from the super long-range seismic profile Quartz. Bulletin of Seismological Society of America 86 (3), 857–867.
Ryzhiy, B.P., Druzhinin, V.S., Yunsov, F.F., Ananyin, I.V., 1992. Deep structure of the Urals region and its seismicity. Physics of the Earth and Planetary Interiors 75, 185–191.
Salmon, M., Kennett, B.L.N., Stern, T., Aitken, A.R.A., 2013. The Moho in Australia and New Zealand. Tectonophysics 609, 288–298 (this volume).
Salnikov, A.S., 2008. Seismic structure of the earth's crust for platform's and folded areas of the Siberia from the data of the regional seismic studies by the refracted waves (Doctor. Sci Dissertation, Novosibirsk).
Salnikov, A.S., Efimov, A.S., Solovyev, V.M., 2012. Deep structure of the crust of Eastern Eurasia based on deep seismic sounding data. Proc. 33rd Gen. Ass. European Seismological Commission, Moscow.
Sandrin, A., Thybo, H., 2008. Seismic constraints on a large mafic intrusion with implications for the subsidence history of the Danish Basin. Journal of Geophysical Research-Solid Earth 113. http://dx.doi.org/10.1029/2007JB005067.
Savinsky, K.A., 1972. Deep Structure of the Siberian Platform Based on Geophysical Data. Nedra, Moscow (242 pp., in Russian).
Schueller, W., Morozov, I.B., Smithson, S.B., 1997. Crustal and uppermost mantle velocity structure of northern Eurasia along the profile quartz. Bulletin of Seismological Society of America 87 (2), 414–426.
Semikhatov, M.A., 1991. General problems of Proterozoic stratigraphy in the USSR. Soviet Scientific Review, Section B. Geology Reviews.Harwood Acad. Publ.
Sengör, A.M.C., Natal'in, B.A., Butman, V.S., 1993. Evolution of the Altaid tectonic collage and Paleozoic crustal growth in Eurasia. Nature 364, 299–307.
Shatsky, V.S., Buzlukova, L.V., Jagoutz, E., Koz'menko, O.A., Mityukhin, S.I., 2005. Structure and evolution of the lower crust of the Daldyn–Alakit district in the Yakutian diamond province (from data on xenoliths). Russian Geology and Geophysics 46, 1273–1289.
Shipilov, E.d.V., Tarasov, G.A., 1998. Regional Geology of Oil and Gas Bearing Sedimentary Basins of the Russian West-Arctic shelf. Apatity, Russia (in Russian).
Sklyarov, E.V., Gladkochub, D.P., Mazukabzov, A.M., Stanevich, M.A., Donskaya, T.V., Konstantinov, K.M., Sinzov, A.V., 2001. Indicator Complexes of Supercontinent Rodinia Break up: Geological Excursion Guide of Workshop 'Supercontinents and geological evolution of Precambrian'. Institute of the Earth Crust SB RAS, Irkutsk 75 (in Russian).
Sokolov, B.A. (Ed.), 1989. Geological-geochemical conditions of formation of oil and gas fields in ancient rocks of East Siberia. Mos-cow University Press, Moscow (192 pp.).
Sokolov, V.B., 1993. Crustal structure of the Urals. Geotectonics 5 (26), 357–366.
Solodilov, L.N., 1997. The GEON centre: 25 years of implementation of PNE in studies of earth's deep structure. In: Fuchs, K. (Ed.), Upper Mantle Heterogeneities From Active and Passive Seismology. Kluwer Academic Publisher, Netherlands, pp. 1–10.
Steer, D.N., Knapp, J.H., Brown, L.D., Rybalka, A.V., Sokolov, V.B., 1995. Crustal structure of the Middle Urals based on reprocessing of Russian seismic reflection data. Geophysical Journal International 123, 673–682.
Steer, D.N., Knapp, J.H., Brown, L.D., Echtler, H.P., Péréz-Estaun, A., Berzin, R., 1998. Deep structure of the continental lithosphere in an unextended orogen: an explosive source seismic reflection profile in the Urals (Urals Seismic Experiment and Integrated Studies (URSEIS 1995)). Tectonics 17, 143–157.
Suleimanov, A.K., 2006. CDP studies for the URSEIS profile. Structure and Dynamics of the East European Lithosphere, v.2. Geokart, GEOS, Moscow, pp. 363–373 (in Russian).
Sultanov, D.D., Murphy, J.R., Rubinstein, Kh.D., 1999. A seismic source summary for Soviet peaceful nuclear explosions. Bulletin of Seismological Society of America 89 (3), 640–647.
Surkov, V.S., Smirnov, L.V., 2003. Basement structure of the oil- and gas-hosting West-Siberian Basin. Otechestvennaya Geologiya 1, 10–16 (in Russian).
Surkov, V.S., Zhero, O.G., 1981. Basement and Development of the Platform Cover of the West Siberian Platform. Nedra, Moscow.
Surkov, V.S., Kuznecov, V.L., Starocelcev, B.S., Salnikov, A.S., 2000. Seismic tomography for study of the crust of Siberia. Regional Geology and Metallogeny 10, 117–124.
Suvorov, V.D., 1993. Deep Seismic Surveys in the Yakutia Kimberlite Province. NAUKA, Novosibirsk.
Suvorov, V.D., Parasotka, B.S., Chernyi, S.D., 1999. Deep seismic sounding studies in Yakutia (Translated from Fizika Zemli, 7–8, 94–113). Izvestiya Physics of the Solid Earth 35 (8), 612–629.
Suvorov, V.D., Melnik, E.A., Manakov, A.V., 2005. Deep structure of the Daldin–Alakit kimberlite area from the results of new interpretation of the data DSS and gravity modeling for the seismic profile Morkoka river–Muna river (Eats Yakutia), 35–47. Izvestiya, Physics of the Solid Earth 5, 35–47.
Suvorov, V.D., Melnik, E.A., Thybo, H., Perchuc, E., Parasotka, B.S., 2006. Seismic velocity model of the crust and uppermost mantle around the Mirnyi kimberlite field in Siberia. Tectonophysics 420, 167–185.
Thouvenot, F., Kashubin, S.N., Poupinet, G., Makovsky, V.V., Kashubina, T.V., Matte, P., Jenatton, L., 1995. The root of the Urals: evidence from wide-angle reflection seismics. Tectonophysics 250, 1–13.
Thybo, H., Artemieva, I.M., 2013. Moho and magmatic underplating in continental lithosphere. Tectonophysics 609, 605–619 (this volume).
Thybo, H., Nielsen, C.A., 2009. Magma-compensated crustal thinning in continental rift zones. Nature 457, 873–876.
Thybo, H., Maguire, P.K.H., Birt, C., Perchuc, E., 2000. Seismic reflectivity and magmatic underplating beneath the Kenya Rift. Geophysical Research Letters 27, 2745–2748.
Thybo, H., Nielsen, L., Perchuc, E., 2003. Seismic scattering at the top of the mantle Transition Zone. Earth and Planetary Science Letters 216, 259–269.
Thybo, H., Ross, A.R., Egorkin, A.V., 2003. Explosion seismic reflections from the Earth's core. Earth and Planetary Science Letters 216, 693–702.
Uarov, V.F., 1981. Seismic peculiarities of the upper mantle of Western Yakutia. Journal of Geology and Geophysics 9, 120–124.
Vernikovsky, V.A., 1996. Geodynamic Evolution of Taimyr Fold Area. SPC UIGGM Siberian Branch RAS, Novosibirsk (In Russian).
Vernikovsky, V.A., Vernikovskaya, A.E., Sal'nikova, E.B., Kotov, A.B., Kovach, V.P., 2003. Neoproterozoic accretion-collisional events on the western margin of the Siberian Craton: new geological and geochronological evidence from the Yenisey Ridge. Tectonophysics 375 (4), 147–168.
Vol'vovsky, I.S., Vol'vovsky, B.S., 1975. Cross-sections of the earth's crust on the territory of the USSR by deep seismic sounding data (1950–1970). Soviet Radio, Moscow.
Vyssotski, A.V., Vyssotski, V.N., Nezhdanov, A.A., 2006. Evolution of the West Siberian Basin. Marine and Petroleum Geology 23, 93–126.
Wang, Q., Ji, S., Salisbury, M.H., Xia, B., Pan, M., Xu, Z., 2005. Pressure dependence and anisotropy of P-wave velocities in ultrahigh-pressure metamorphic rocks from the Dabie–Sulu orogenic belt (China): implications for seismic properties of subducted slabs and origin of mantle reflections. Tectonophysics 398, 67–99.
White, R.S., Smith, L.K., Roberts, A.W., Christie, P.A.F., Kusznir, N.J., 2008. Lower-crustal intrusion on the North Atlantic continental margin. Nature 452, 460–465.
Wooden, J.L., Czamanske, G.K., Fedorenko, V.A., Arndt, N.T., Chauvel, C., Bouse, R.M., King, Bi-Shia W., Knight, R.J., Siems, D.F., 1993. Isotopic and trace-element constraints on mantle and crustal contributions to Siberian continental flood basalts, Noril'sk area, Siberia. Geochimica et Cosmochimica Acta 57 (15), 3677–3704.

Youssof, M., Thybo, H., Levander, A., Artemieva, I., 2012. Why is the Kaapvaal different from other cratons? Geophysical Research Abstracts 14 (EGU 2012-8761-3).
Youssof, M., Thybo, H., Artemieva, I.M., Levander, A., 2013. Moho depth and crustal composition in the Southern Africa. Tectonophysics 609, 267–287 (this volume).
Zhao, G., Cawood, P.A., Wilde, S.A., Sun, M., 2002. Review of global 2.1–1.8: Ga orogens: implications for a pre-Rodinia supercontinent. Earth-Science Reviews 59, 125–162.
Zhuravlev, E.G., 1986. The trap formation of the West Siberian plate. Izvestya Akademii Nauk SSSR. Seriya Geograficheskaya 7, 26–32.
Zonenshain, L., Kuzmin, M.I., Natapov, L.M., 1990. Geology of the U.S.S.R.: A Plate Tectonic Synthesis. American Geophysical Union.
Zorin, Yu.A., Belichenko, V.G., Turutanov, E.Kh., Mazukabzov, A.M., Slkyarov, E.V., Mordvinova, V.V., 1995. The East Siberian transect. International Geology Review 37, 154–175.
Zorin, Y.A., Mordvinova, V.V., Turutanov, E.K., Belichenko, B.G., Artemyev, A.A., Kosarev, G.L., Gao, S.S., 2002. Low seismic velocity layers in the Earth's crust beneath Eastern Siberia (Russia) and Central Mongolia: receiver function data and their possible geological implication. Tectonophysics 359, 307–327.
Zorin, Y.A., Turutanov, E.Kh., Mordvinova, V.V., Kozhevnikov, V.M., Yanovskaya, T.B., Tressov, A.V., 2003. The Baikal Riftzone: the effect of mantle plumes on older structure. Tectonophysics 371, 153–173.
Zverev, S.M., Kosminskaya, I.P., 1980. Seismic models of the lithosphere for the major geostructures on the territory of the USSR. NAUKA, Moscow.